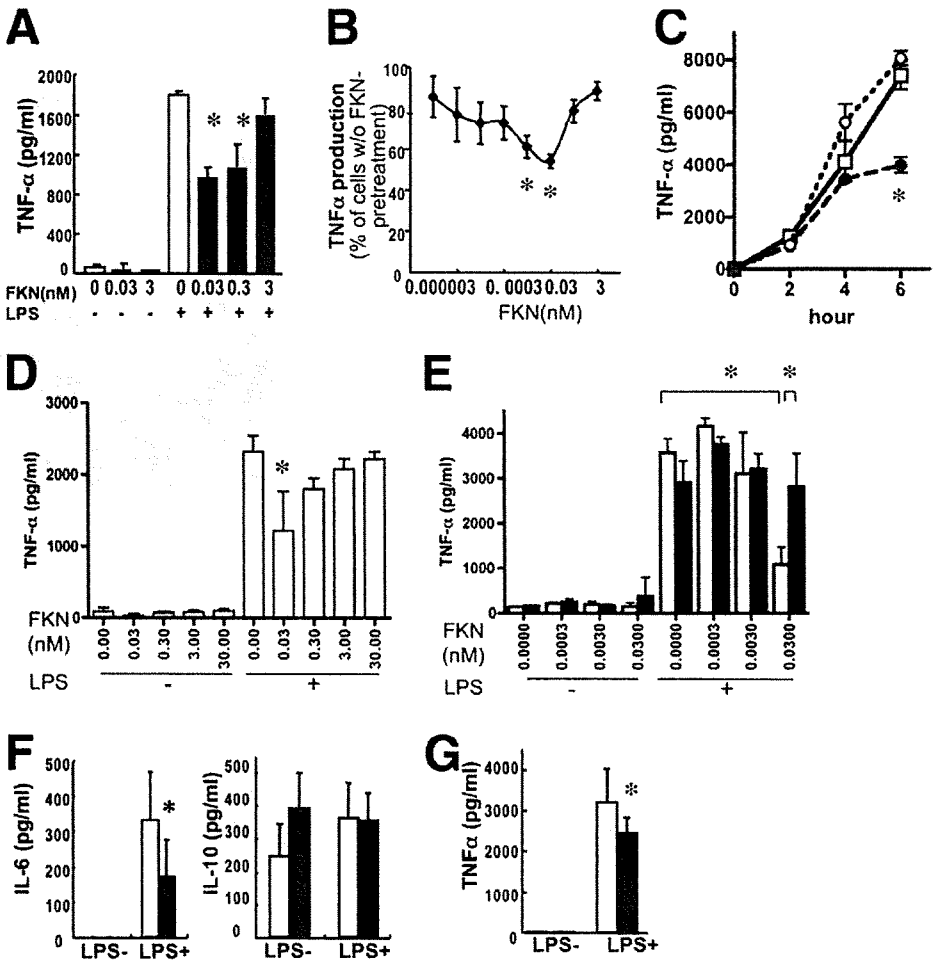

FIGURE 2. Pretreatment with recombinant FKN inhibited LPS-induced TNF-α production in macrophages. *A*, BMϕ were pretreated with FKN at indicated concentrations for 12 h and stimulated with LPS (100 ng/ml) for 6 h. Secretion of TNF-α in the culture medium was determined by ELISA and shown as an average plus 1 SD of four to eight independent cell preparations. *B*, RAW264.7 cells were pretreated with FKN at the indicated concentration for 12 h and stimulated with LPS (1 ng/ml) for 6 h. Secretion of TNF-α in the culture medium was determined by ELISA and shown as an average ± 1 SD of the percentage of cells without FKN pretreatment using three to eight independent cultures. *C*, RAW264.7 cells were pretreated with 0 nM (□), 0.03 nM (●), or 3 nM (○) FKN for 12 h and stimulated with LPS (1 ng/ml). Secretion of TNF-α in the culture medium was determined by ELISA at the indicated times after LPS stimulation and are shown as the average plus 1 SD. *D*, Culture plates were coated with indicated concentrations of FKN and RAW264.7 cells were cultured for 12 h and stimulated with LPS (1 ng/ml) for 6 h. Secretion of TNF-α was measured and shown as the average of eight cultures plus 1 SD. *E*, RAW264.7 cells were pretreated with FKN at the indicated concentrations in the presence of anti-CX3CR1 Ab (■ or control IgG (□) for 12 h and stimulated with LPS (1 ng/ml) for 6 h. Secretion of TNF-α was measured and shown as the average of three cultures plus 1 SD. *F*, BMϕ were pretreated with (■) or without (□) 0.03 nM FKN and then stimulated with 100 ng/ml LPS for 6 h. Secretions of IL-6 and IL-10 were measured and shown as an average plus 1 SD. *G*, BMϕ prepared from IL-10$^{-/-}$ mice (n = 10) were pretreated with (■) or without (□) 0.03 nM FKN and stimulated with 100 ng/ml LPS. Secretion of TNF-α was measured and shown as an average plus 1 SD. *, Statistically significant difference from cells without FKN- pretreatment; otherwise, compared data are indicated ($p < 0.05$).

CX3CR1, a forward primer (5′-CCGCCAACTCCATGAACAA) and a reverse primer (CGTCTGGATGATGCGGAAGTA-3′); PPAR-γ, a forward primer (5′-GATGCAAGGGTTTCTTCCGGAGAAC) and a reverse primer (TGGTGATTTGTCTGTTGTCTTTCC-3′); IL-23 p19, a forward primer (5′-GAACAAGATGCTGGATTGCAGAG) and a reverse primer (TGTGCGTTCCAGGCTAGCA-3′); and GAPDH, a forward primer (5′-AGCCAAACGGGTCATCATCTC) and a reverse primer (TGCCTGCT TCACCACCTTCTT-3′). For quantitative analysis, the SYBR Green PCR Kit (Applied Biosystems) was used according to the manufacturer's instructions in a model 7700 Sequence Detector (Applied Biosystems). The reaction mixture was amplified for GAPDH (95°C for 45 s, 60°C for 45 s, and 72°C for 45 s, in the order of denaturation, annealing, and extension, 40 cycles); MD-2 (90°C for 45 s, 58°C for 45 s, 72°C for 45 s, 40 cycles); TLR4 (94°C for 60 s, 60°C for 60 s, 72°C for 60 s, 40 cycles); CX3CR1 (94°C for 45 s, 58°C for 45 s, 72°C for 45 s, 40 cycles); FKN (94°C for 45 s, 58°C for 45 s, 72°C for 45 s, 40 cycles); PPAR-γ (95°C for 45 s, 55°C for 45 s, 72°C for 45 s, 40 cycles); and IL-23 p19 (95°C for 45 s, 60°C for 45 s, 72°C for 45 s, 40 cycles).

Preparation of nuclear extracts and EMSA

Cells were suspended in 200 μl of lysis buffer (10 mM HEPES (pH 7.9), 10 mM KCl, 0.1 mM EDTA, 0.1 mM EGTA, and 1 mM DTT) and kept on ice for 15 min followed by addition of 12.5 μl of 10% Nonidet P-40. After mixing and centrifugation (10,000 × g) for 3 min, the nuclear pellets obtained were resuspended in 25 μl of ice-cold nuclear extraction buffer (20 mM HEPES (pH 7.9), 400 mM NaCl, 1 mM EDTA, 1 mM EGTA, and 1 mM DTT) and kept on ice for 15 min with intermittent agitation. The samples were centrifuged and the supernatants were stored at −80°C until use. EMSAs were conducted using a Digoxigenin Gel Shift Kit (Roche Diagnostics) according to the manufacturer's instructions using 10 μg of the nuclear extracts. Quantification of bands was performed by densitometry using ATTO Densitograph version 4.0 software. For the supershift assay, we used an identical oligonucleotide probe labeled with [^{32}P]dCTP using a Klenow fragment. In brief, nuclear extracts (3 μg) were preincubated with 1 μg of anti-p50 or p65 Ab (sc-1190X, sc-372X; Santa Cruz Biotechnology) for 60 min at 4°C before addition of the labeled probe in

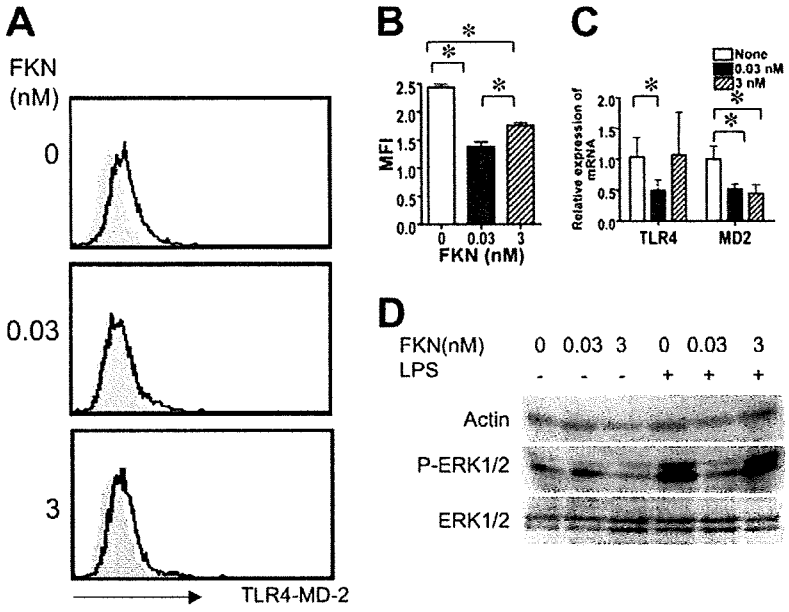

FIGURE 3. Pretreatment with FKN altered TLR4 and MD-2 expression and ERK1/2 phosphorylation. *A*, RAW264.7 cells were pretreated with the indicated concentrations of FKN for 12 h and stained with an Ab against the TLR4-MD-2 complex. Shaded histograms indicate staining with isotype control. *B*, The results in *A* are shown as the difference in mean fluorescence intensity from that of the isotype control. Results are shown as an average plus 1 SD of three experiments. *C*, RAW264.7 cells were pretreated with the indicated concentrations of FKN for 12 h and subjected to quantitative RT-PCR for TLR4 and MD-2. Results are shown as an average ($n = 3$ cultures) plus 1 SD of relative expression compared with the level of cells without FKN pretreatment. *, Statistically significant difference from cells without FKN pretreatment ($p < 0.05$). *D*, RAW264.7 cells were pretreated with the indicated concentration of FKN for 12 h and stimulated with LPS (1 ng/ml). Cell extracts were obtained after a 12-h pretreatment with FKN (LPS−) or after additional stimulation with LPS for 6 h (LPS+). Extracts were subjected to Western blotting to detect actin, phoshpo-ERK1/2, MAPK, and total ERK1/2. Representative data from four separate experiments are shown.

a total of 25 μl of binding buffer (10 mM HEPES (pH 7.8), 50 mM KCl, 1 mM EDTA, 5 mM MgCl2, 10% glycerol, and 1 μg of poly(dI:C)). After incubation, samples were fractionated on a 5% polyacrylamide gel in 25 mM Tris-Cl (pH 8.5), 190 mM glycine, and 1 mM EDTA. The gel was subsequently dried and visualized by autoradiography.

Quantification of NF-κB p65

The amount of NF-κB p65 in the nuclear protein fraction was measured using the TransFactor Extraction Kit and TransFactor Colorimetric Kit for NF-κB (BD Clontech). Amounts of NF-κB p65 were quantified as arbitrary units based on the colorimetric assay of serial dilutions of positive control samples.

Cell staining for detection of PPAR-γ and NF-κB p65

RAW264.7 cells were plated on Lab-Tek Chamber Slides (Nalge Nunc). After experimental treatment, cells were fixed by methanol, blocked with Block Ace (Dainippon Seiyaku) for 1 h, and incubated with rabbit anti-NF-κB p65 Ab (sc-372; Santa Cruz Biotechnology) and mouse anti-PPAR-γ mAb (sc-7273; Santa Cruz Biotechnology) or control normal mouse IgG (Cedarlane Laboratories) and normal rabbit IgG (Santa Cruz Biotechnology). Bound Ab were detected with goat anti-rabbit IgG tetramethylrhodamine isothiocyanate (Southern Biotechnology Associates) or biotinylated anti-mouse IgG (Vector Laboratories) and streptavidin-Alexa 488 (Invitrogen Life Technologies and Molecular Probes). Cells were then analyzed by confocal laser scanning microscopy (Zeiss LSM510; Zeiss).

Small interfering RNA (siRNA)

siRNA for mouse PPAR-γ and control siRNA were purchased from Santa Cruz Biotechnology. RAW264.7 cells were transfected with double-stranded siRNA at a final concentration of 100 nM using the MicroPorator MP-100 electroporation system (Digital BioTechnology) according to the manufacturer's instructions.

Immunostaining for 15d-PGJ2

RAW264.7 cells were stained with 2 μg/ml mouse anti-15d-PGJ2 mAb (11G2) or mouse control IgG overnight at 4°C as described previously (36) and then incubated with biotinylated anti-mouse IgG at a 1/400 dilution (Vector Laboratories) for 1 h followed by streptavidin-Alexa 488 at 1/1000 dilution for 1 h. After final washing and counterstaining with 4′,6-diamidino-2-phenylindole (DAPI), samples were evaluated using fluorescence microscopy (BX50/BXFLA; Olympus). Green (15d-PGJ2) and blue (nuclei) fluorescence images were captured separately from four fields of each culture randomly, and the stained area was measured using ImageJ software (distributed by the National Institutes of Health). Cellular expression of 15d-PGJ2 was determined as the green area (pixels) divided by blue area (pixels), which represents the number of cells in the image.

Statistics

The results were compared by the Mann-Whitney *U* test using the StatView II statistical program (Abacus Concepts) adapted for Mac OS.

Results

FKN and CX3CR1 are abundantly expressed in the intestine

Since CX3CR1-positive dendritic cells are abundantly distributed in the lamina propria of normal intestine (27), we initially examined the expression of the FKN ligand in the intestine. FKN was detected in epithelial as well as mesenchymal cells, especially in the proximal colon (Fig. 1*A*). FKN-positive mesenchymal cells, including myofibroblasts, were identified by double staining with anti-αsmooth musele actin as well as RT-PCR of murine myofibroblast cell lines which were established from the colon (our unpublished data). $CX3CR1^+F4/80^+$ macrophages were also found more frequently in the colon compared with the small intestine (Fig. 1*B*).

FKN attenuated LPS-induced secretion of TNF-α

To investigate the effect of FKN, we chose BMϕ and the mouse macrophage cell line RAW264.7 because both express the FKN receptor CX3CR1 (92 and 90%, respectively) and produce large amounts of TNF-α, an indicator of inflammation, in response to LPS stimulation for 6 h (Fig. 2). These cells were pretreated with FKN for 12 h and then stimulated with LPS. Although FKN itself did not induce secretion of TNF-α, pretreatment with FKN reduced the secretion of LPS-induced TNF-α in both BMϕ and RAW264.7 cells (Fig. 2, *A* and *B*). Of interest, ~0.003–0.03 nM FKN was optimal for this effect, and a higher concentration (3 nM) of FKN failed to attenuate TNF-α secretion (Fig. 2, *A* and *B*). Addition of an anti-FKN Ab during FKN pretreatment (0.03 nM) abolished its inhibitory effect, which indicated that the effect was due to FKN rather than any minor contaminant (data not shown). In the time course assay, less secretion of TNF-α in cells pretreated with 0.03 nM FKN became obvious 6 h after LPS challenge (Fig. 2*C*). Since FKN is expressed as a membrane-bound molecule as well as a soluble protein, we immobilized FKN on a plate and cultured RAW264.7 cells before LPS challenge. Immobilized FKN at a concentration of 0.03 nM also showed decreased TNF-α production by macrophages in response to LPS, whereas higher

concentrations did not show this effect (Fig. 2*D*). Washing the cells before LPS challenge reduced, at least in part, the inhibitory effect of FKN on TNF-α (data not shown), which indicated that both intracellular events and soluble factors released during pretreatment were involved in inhibition. To confirm that these dose-dependent, differential effects were mediated by a single FKN receptor, we added anti-CX3CR1 Ab when cells were pretreated with FKN. Reduction of TNF-α secretion in cells pretreated with 0.03 nM FKN was negated in the presence of anti-CX3CR1 Ab (Fig. 2*E*). This result indicated that the TNF-α suppressive effect was mediated by CX3CR1.

Pretreatment with 0.03 nM FKN also suppressed secretion of IL-6 from BMϕ induced by LPS, although the inhibitory effect was not as evident as that observed with levels of TNF-α in a 6-h culture (Fig. 2*F*). IL-12 production also was induced by LPS in BMϕ, but pretreatment with FKN did not affect its secretion significantly (data not shown). BMϕ constitutively produced IL-10 and pretreatment with FKN did not alter the levels of IL-10 in the culture supernatant, either without or with LPS (Fig. 2*F*). Similar effects of FKN pretreatment on cytokine production were seen in RAW264.7 cells. To examine the possible involvement of IL-10, BMϕ prepared from IL-$10^{-/-}$ mice were tested. Levels of TNF-α secretion after LPS stimulation in IL-$10^{-/-}$ BMϕ were >2-fold higher than in wild-type mice; however, pretreatment with FKN significantly decreased the level of TNF-α, although it did not reach 50% inhibition as seen in wild-type mice (Fig. 2*G*). Overall results showed that the LPS-induced TNF-α response was suppressed by pretreatment with 0.03 nM FKN and involvement of IL-10 in TNF-α suppression was only partial, if at all.

Pretreatment with FKN-modulated expression of TLR4

We next investigated whether FKN pretreatment might alter the expression of TLR4 and MD-2, molecules necessary for signal transduction from LPS. Although cell surface expression of the TLR4-MD-2 complex was not high in RAW264.7 cells, it significantly decreased in cells pretreated with 0.03 nM FKN as determined by flow cytometry (Fig. 3, *A* and *B*). Levels of TLR4 and MD-2 mRNA also decreased after pretreatment with 0.03 nM FKN (Fig. 3*C*). However, the mean fluorescence intensity of TLR4-MD-2 and mRNA levels of MD-2 in the cells treated with 3 nM FKN was still significantly lower than that of untreated control cells. Since TNF-α production by cells treated with 3 nM FKN was comparable to that of untreated cells, we assume that the surface expression level of TLR4-MD-2 was not the major factor that directly caused suppression of TNF-α secretion, although FKN does affect TLR4-MD-2 expression.

FKN attenuated ERK1/2 activation

Since MAPK phosphorylation occurs downstream of TLR4 signaling, the effect of FKN pretreatment was assessed. FKN itself induced ERK1/2 phosphorylation within 30 min; however, after 12 h (the time point of LPS addition), there was no significant activation of ERK1/2 in cells treated with either concentration of FKN (Fig. 3*D*). Phosphorylation of ERK1/2 was detected 30 min after stimulation with LPS irrespective of pretreatment with FKN (data not shown); however, 6 h after LPS challenge, MAPK phosphorylation was dramatically suppressed when cells were pretreated with 0.03 nM FKN. A higher concentration of FKN (3 nM) did not inhibit ERK phosphorylation (Fig. 3*D*), coinciding with the failure to suppress TNF-α secretion at this concentration. Phosphorylation of p38 was seen after stimulation with LPS; however, there is no difference between cells with or without FKN pretreatment (data not shown).

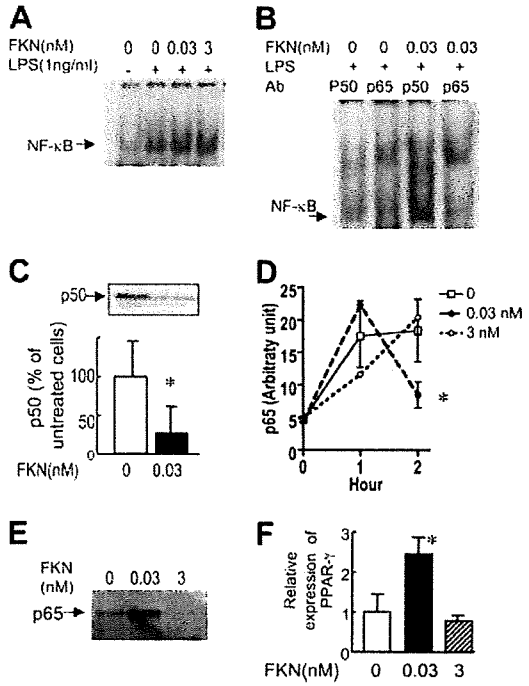

FIGURE 4. Pretreatment with FKN modulated activation of NF-κB. *A*, RAW264.7 cells were pretreated with the indicated concentration of FKN for 12 h and stimulated with LPS for 1 h. Nuclear extracts were subject to EMSA using a consensus NF-κB oligonucleotide probe. Specificity was confirmed by the loss of this band with the addition of unlabeled probe as a competitor. *B*, RAW264.7 cells were pretreated with or without 0.03 nM FKN and stimulated with 1 ng/ml LPS for 1 h. Nuclear extracts were subjected to supershifted EMSA in the presence of anti-NF-κB p65 or anti-p50 Ab. *C*, RAW264.7 cells were pretreated with 0.03 nM FKN and stimulated with 1 ng/ml LPS. Nuclear extracts were subject to Western blotting to detect p50 (*top panel*). The amount of p50 protein in three sets of experiments was quantified by densitometry and shown as the mean plus 1 SD normalized to the samples without pretreatment. *, Statistically significant difference from untreated cells ($p < 0.05$). *D*, RAW264.7 cells were pretreated with the indicated concentration of FKN for 12 h and stimulated with LPS for 1 or 2 h. Levels of p65 in the nuclear extract were measured. Results are shown as an average of eight independent cultures plus 1 SD. *, Statistically significant difference from untreated cells or cells treated with 3 nM FKN ($p < 0.05$). *E*, RAW264.7 cells were pretreated with the indicated concentration of FKN and stimulated with 1 ng/ml LPS for 2 h. Cytoplasmic extracts were immunoprecipitated with anti-PPAR-γ mAb and then subjected to blotting with anti-p65 Ab. *F*, RAW264.7 cells were pretreated with the indicated concentration of FKN for 12 h and mRNA extracts were subjected to RT-PCR for PPAR-γ. Results are shown as an average plus 1 SD of relative expression compared with the levels of nonpretreated cells from three independent preparations. *, Statistically significant difference from untreated cells or cells treated with 3 nM FKN ($p < 0.05$).

Effect of FKN pretreatment on NF-κB activation and induction of PPAR-γ

Inflammatory responses are closely linked to the activation of NF-κB, and LPS-induced transcription of TNF-α in macrophages is highly dependent on nuclear translocation of NF-κB. When RAW264.7 cells were stimulated with LPS, NF-κB activation was seen (Figs. 4*A* and 5*A*). Without LPS, very low levels of nuclear NF-κB were detected in RAW264.7 cells and treatment with either 0.03 nM or 3 nM FKN alone for 12 h did not show a significant effect on the status of NF-κB (data not shown). Unexpectedly, pretreatment with 0.03 nM FKN did not alter the amount of nuclear-translocated κB-binding protein for 1 h after LPS challenge

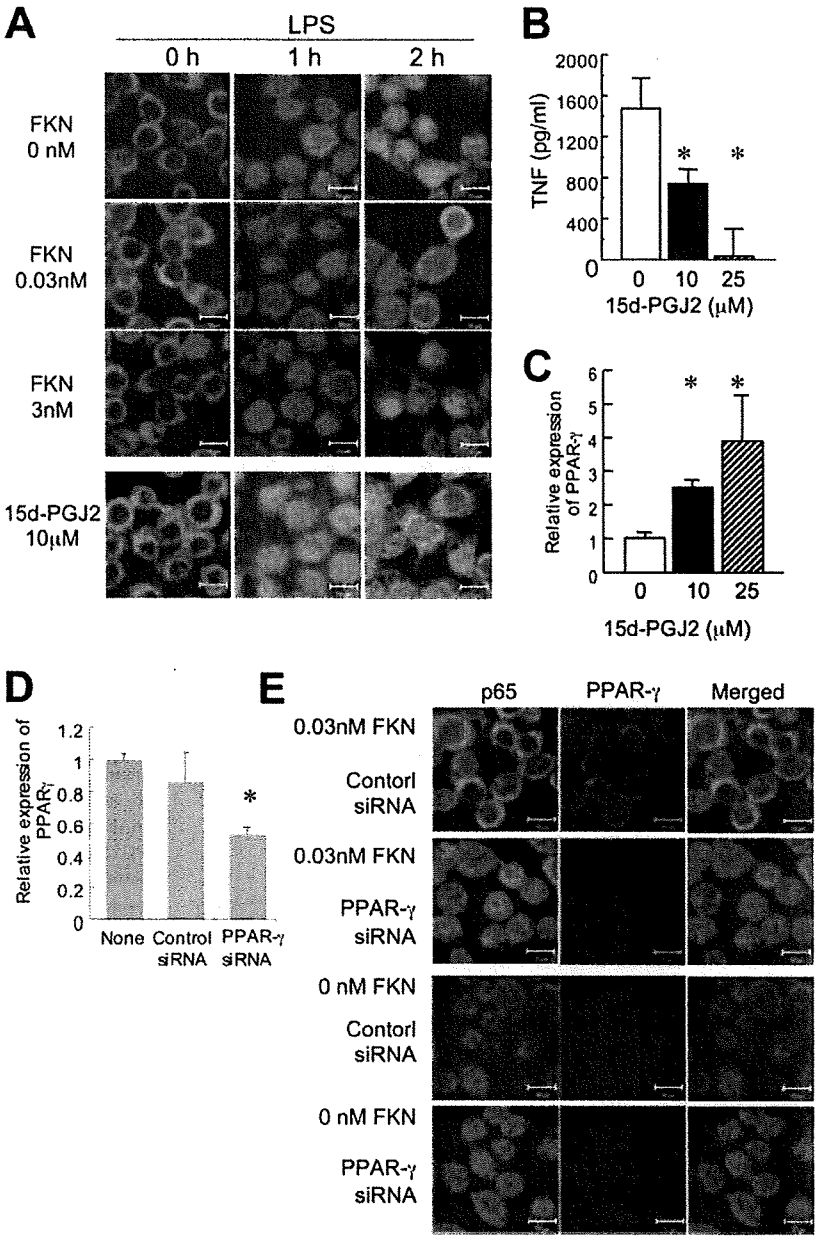

FIGURE 5. Pretreatment with FKN induced early export of NF-κB p65 from nuclei after stimulation with LPS in a PPAR-γ-dependent manner. *A*, RAW264.7 cells were pretreated with or without the indicated concentrations of either FKN or 15d-PGJ2 for 12 h and stimulated with 1 ng/ml LPS for either 1 or 2 h. Cells were then stained with anti-p65 (red) and anti-PPAR-γ (green) Ab; the merged images are shown. One representative result from four independent cultures in each condition is shown. *B*, RAW264.7 cells were pretreated with the indicated concentrations of 15d-PGJ2 for 12 h and stimulated with 1 ng/ml LPS for 6 h. Culture supernatants were subjected to TNF-α ELISA. Results are shown as the average plus 1 SD of four independent preparations. *C*, RAW264.7 cells were pretreated with the indicated concentrations of 15d-PGJ2 for 12 h and RNA extracts were subjected to quantitative RT-PCR for PPAR-γ. Results are shown as the mean plus 1 SD of the relative expression of the levels of nonpretreated cells of three independent preparations. *, Statistical significant differences from control cells without pretreatment. *D*, RAW264.7 cells were transfected with either PPAR-γ siRNA or control siRNA. Thirty-six hours after siRNA transfection, cells were treated with 0.03 nM FKN for 12 h. Total RNA was isolated and the levels of PPAR-γ mRNA were determined by quantitative RT-PCR. The fold induction was shown as the mRNA level relative to that of cells without siRNA transfection. Results are shown as the mean plus 1 SD of relative expression of the levels of nonpretreated cells from six independent preparations. *, Statistical significant differences from cells without transfection or transfected with control siRNA. *E*, RAW264.7 cells were transfected with either PPAR-γ or control siRNA. Thirty-six hours after transfection, cells were precultured with 0.03 nM FKN or without FKN (0 nM) for 12 h and then stimulated with 1 ng/ml LPS for 2 h. Cells were stained with anti-p65 (red) and anti-PPAR-γ (green) Ab. Representative results from four independent cultures in each condition are shown.

(Fig. 4*A*). Therefore, to find the mechanism of decreased TNF-α production, we performed supershift analysis focusing on the effect of pretreatment with 0.03 nM FKN. Without pretreatment, supershift was seen with both anti-p65 and anti-p50 Ab. In contrast, when cells were pretreated with 0.03 nM FKN, clear supershift was not seen with the anti-p50 Ab, while the NF-κB complex was supershifted with the anti-p65 Ab (Fig. 4*B*).

Decreased nuclear translocation of p50 protein in FKN-pretreated cells was confirmed by Western blotting (Fig. 4*C*). Furthermore, pretreatment with 0.03 nM FKN did not reduce but rather slightly increased the levels of p65 protein in the nucleus compared with those of untreated cells at the time point of 1 h after stimulation with LPS (Figs. 4*D* and 5*A*). Importantly, in these FKN-pretreated cells, p65 was rapidly eliminated from the nuclei 2 h after addition of LPS (Figs. 4*D* and 5*A*). In contrast, p65 remained in the nuclei at this time point in cells either without pretreatment or pretreated with 3 nM FKN (Figs. 4*D* and 5*A*).

From these results, we assumed that when cells were pretreated with 0.03 nM FKN, NF-κB p65 did not form a complex with p50 but with other molecules, which facilitated transport of p65 protein out of the nucleus. Since PPAR-γ was previously reported to have such a function (37), we performed immunoprecipitation analysis. We found that p65 protein and PPAR-γ were coprecipitated from cytoplasmic fractions 2 h after stimulation with LPS in cells that had been pretreated with 0.03 nM FKN (Fig. 4*E*). However, when cells were pretreated with 3 nM FKN, the p65-PPAR-γ complex was not detected (Fig. 4*E*). Immunofluorescence analysis also showed that nuclear p65 was efficiently moved to the cytoplasm with PPAR-γ in the cells pretreated with 0.03 nM FKN, while p65 remained in the nuclei in the cells without treatment or pretreated with 3 nM FKN 2 h after LPS stimulus (Fig. 5*A*). Since PPAR-γ is known to be a negative regulator of the inflammatory cytokine responses of macrophages (38, 39), we postulated that pretreatment with 0.03 nM FKN would induce and activate PPAR-γ and modulate NF-κB translocation, and finally attenuate the secretion of TNF-α. To examine this possibility, we determined the mRNA levels of PPAR-γ and found that the levels were enhanced after

a 12-h treatment with 0.03 nM FKN when compared with non-treated cells or those treated with 3 nM FKN (Fig. 4*F*).

Exogenous PPAR-γ ligand mimicked the effect of FKN

Since our results indicated the role of PPAR-γ activation in the anti-inflammatory effect of FKN, we pretreated cells with a natural PPAR-γ ligand and agonist, 15d-PGJ_2, instead of FKN. Pretreatment of RAW264.7 cells with 10 μM 15d-PGJ2 resulted in enhanced expression of PPAR-γ and nuclear translocation of p65 1 h after LPS stimulation, and then the p65 was rapidly cleared from nuclei at 2 h, as was observed in cells pretreated with 0.03 nM FKN (Fig. 5*A*). As a result, secretion of TNF-α decreased to 50% of untreated cells when cells were pretreated with 10 μM 15d-PGJ2 (Fig. 5*B*). The overall effect seen in the cells pretreated with 10 μM 15d-PGJ2 was similar to the effect of pretreatment with 0.03 nM FKN. Furthermore, we found that exogenous 15d-PGJ2 up-regulated PPAR-γ mRNA expression (Fig. 5*C*).

Effect of FKN on p65 redistribution depends on PPAR-γ

To confirm the key role of PPAR-γ in the effect of FKN on p65 redistribution, we used RNA interference. The introduction of siRNA for mouse PPAR-γ into RAW264.7 cells resulted in a 50% decrease in PPAR-γ mRNA levels compared with cells treated with control siRNA as determined by quantitative RT-PCR (Fig. 5*D*). As a result, PPAR-γ expression decreased (Fig. 5*E*) and the effect of pretreatment with 0.03 nM FKN was abolished; the NF-κB p65 subunit was retained in the nuclei 2 h after LPS challenge (Fig. 5*E*).

FKN enhances the levels of 15d-PGJ2

The exogenous PPAR-γ ligand 15d-PGJ2 up-regulated PPAR-γ mRNA expression and similarly altered NF-κB activation. Therefore, we investigated whether FKN itself could induce 15d-PGJ2. After a 2-h treatment with 0.03 nM FKN, 15d-PGJ2 was up-regulated and the enhanced expression was maintained for 12 h (Fig. 6, *A* and *B*). In contrast, expression levels of 15d-PGJ2 in cells treated with 3 nM of FKN were not significantly different from untreated control cells.

Induction of IL-23 by high concentrations of FKN

Since both 0.03 and 3 nM FKN showed a distinct effect in macrophages, we compared the mRNA levels of cytokines in cells pretreated with these low and high concentrations of FKN. Although there was no difference in expression of anti-inflammatory cytokines such as TGF-β or IL-10, we found that IL-23 p19 mRNA expression was significantly elevated in cells pretreated with 3 nM FKN and stimulated with LPS in comparison to those in cells not pretreated or pretreated with 0.03 nM FKN (Fig. 7*A*). Since induction of IL-23 p19 by high concentrations of FKN was blocked by anti-CX3CR1-neutralizing Ab, it was assumed to be mediated by CX3CR1 (Fig. 7*A*). Since 0.03 nM FKN as well as 3 nM FKN fully induced chemotaxis (data not shown), we assumed that signal transduction via CX3CR1 was sufficient at this relatively low concentration of FKN, and additional signals that promote IL-23 p19 expression might be induced at a higher concentration of FKN. This hypothesis was supported by the observation that addition of IL-23 after pretreatment with 0.03 nM FKN abolished the suppressive effect of 0.03 nM FKN (Fig. 7, *B* and *C*). Furthermore, early export of NF-κB p65 from the nuclei in the cells pretreated with 0.03 nM FKN was prevented in the presence of IL-23 (Fig. 7*C*). The significance of IL-23 in the action of 3 nM FKN was also supported by experiments using anti-IL-23 Ab. Both secretion of TNF-α and retention of NF-κB p65 in the nuclei after LPS stimulation in cells pretreated with 3 nM FKN were abolished in the presence of anti-IL-23 p19 Ab (Fig. 7, *D* and *E*).

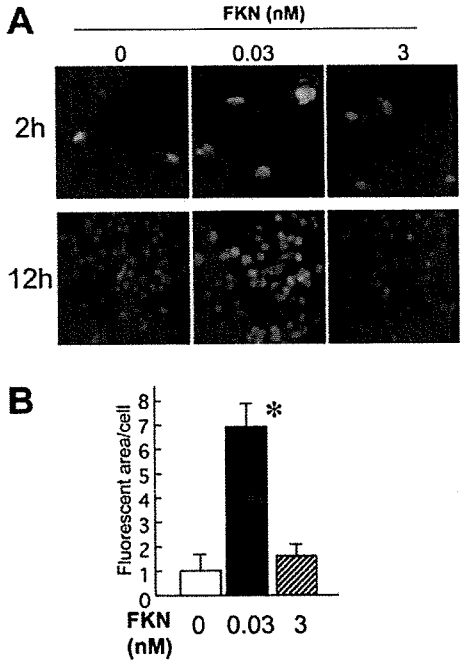

FIGURE 6. FKN increased the level of 15d-PGJ2. *A*, RAW264.7 cells were treated with the indicated concentration of FKN for 2 or 12 h and cells were stained with anti-15d-PGJ2 mAb (green). Nuclei were visualized by staining with DAPI (blue). *B*, RAW264.7 cells were treated with the indicated concentration of FKN for 12 h and stained with anti-15d-PGJ2 mAb and DAPI. The image as in *A* was captured and the levels of 15d-PGJ2 were measured as a ratio of green area to blue area. Results are shown as an average plus 1 SD of four measurements normalized to the value of cells without FKN treatment. Two other sets of experiments gave identical results. *, Statistically significant difference from cells without treatment 0 or treated with 3 nM FKN.

Discussion

This is the first report of an immunomodulatory effect of FKN independent of its well-investigated function as a chemokine and adhesion molecule. The mechanism of the anti-inflammatory effect of relatively low concentrations of FKN involved activation of PPAR-γ by induction of its ligand, 15d-PGJ2, and alteration of signaling via ERK1/2 and NF-κB. These novel immune regulation systems in macrophages are discussed below.

Up-regulation of FKN expression in inflammatory tissue has drawn attention to its potential as a target of anti-inflammatory treatment for various autoimmune diseases. However, FKN is constitutively produced by intestinal epithelial cells and its receptor, CX3CR1, is expressed on tissue-resident dendritic cells and macrophages in the intestine and CNS. In the case of murine intestine, we found that a considerable amount of FKN was expressed in the colon, and colonic myofibroblasts were also another significant source of FKN (our unpublished data). Of note, the resident macrophages of the intestine are hyporesponsive to inflammatory stimuli with bacterial components such as LPS. It is evident, especially in the large intestine, that macrophage-like cells in the colonic lamina propria are mostly anergic in response to endotoxin, in contrast to the vigorous cytokine production by circulating monocyte via the same stimuli (33). For heavy colonization of indigenous Gram-negative bacteria in the colon, hyporesponsiveness of macrophages would be important for maintaining homeostasis of

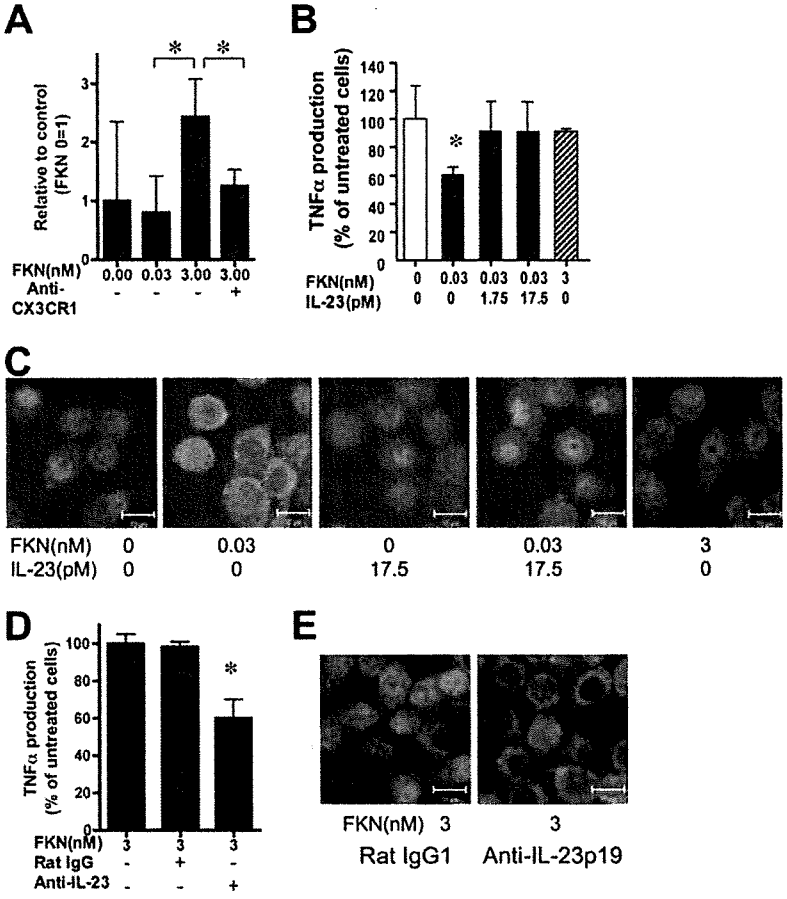

FIGURE 7. Pretreatment with a high concentration of FKN up-regulated mRNA for IL-23 p19 after LPS stimulation and facilitated TNF-α secretion. *A*, RAW264.7 cells were treated with the indicated concentration of FKN for 12 h with or without anti-CX3CR1 Ab or control IgG and stimulated with LPS (1 ng/ml) for 6 h. Cells then were subjected to quantitative RT-PCR for IL-23 p19. *, Indicates that the difference from cells treated with 0.03 nM FKN is statistically significant ($p < 0.05$). *B*, RAW264.7 cells were pretreated with the indicated amount of FKN and then stimulated with LPS in the presence of various amounts of IL-23 for 6 h. Secretion of TNF-α in culture supernatants was measured by ELISA. Results are shown as an average plus 1 SD of the percentage of the value of cells without FKN pretreatment from six independent cultures. *, Statistically significant difference from other experimental conditions shown ($p < 0.05$). *C*, RAW264.7 cells were pretreated with or without 0.03 or 3 nM FKN for 12 h and then stimulated with LPS (0.03 nM) in the absence or presence of IL-23 (17.5 pM) for 2 h. Cells then were stained with anti-p65 (red) and anti-PPAR-γ (green) Ab; the merged images are shown. *D*, RAW264.7 cells were pretreated with 3 nM FKN for 12 h and then stimulated with LPS (1 ng/ml) with or without anti-IL-23 Ab or control IgG for 6 h. Results are shown as the average plus 1 SD of the percentage of cells without FKN pretreatment from six independent cultures. *, Statistically significant difference from other experimental conditions shown ($p < 0.05$). *E*, RAW264.7 cells were pretreated with 3 nM FKN for 12 h and then stimulated with LPS (1 ng/ml) with or without anti-IL-23 Ab for2 h. Cells were then stained with anti-p65 Ab.

mucosal immunity. The possibility that FKN participates in rendering macrophages hyporesponsive to LPS was first demonstrated in this study. This effect of FKN is reminiscent of the phenomenon of endotoxin tolerance, i.e., exposure of macrophages to LPS induces a hyporesponsive state to a second challenge with LPS. Although various mechanisms are involved in endotoxin tolerance, few studies have reported the mechanism of hyporesponsiveness of intestinal macrophages at the molecular level. For example, the IκBNS is a key molecule that inhibits IL-12 and IL-6 production in murine intestinal macrophages, although this mechanism was irrelevant to TNF-α secretion (31). Lack of MD-2 expression in intestinal myeloid-type cells (33) or epithelial cells (40) also has been postulated as a mechanism for the limited responses to LPS derived from indigenous flora. However, in our study, FKN did not down-regulate expression of the TLR4-MD-2 completely, although the level of mRNA was significantly reduced. Furthermore, IL-10 was not entirely responsible for the suppression of TNF-α. We also found that Bcl3 and TNFR-associated factor 6 were not significantly involved in this system (our unpublished data). Thus, the mechanism of inhibition of LPS-triggered TNF-α secretion by FKN was distinct from those mechanisms already known for the phenomenon of endotoxin tolerance.

In the current study, we found that FKN up-regulated PPAR-γ expression with its ligand and reduced production of TNF-α. This was also associated with modulation of subunit usage of NF-κB; the p65 subunit did not form a complex with the p50 subunit as seen in the LPS-challenged cells without FKN pretreatment. Instead, PPAR-γ formed a complex with the p65 subunit, which seemed to facilitate early export of p65 from nuclei. Inhibition of NF-κB activation by cytoplasmic protein IκB, which prevents nuclear translocation of p65, is not likely to be a major factor in the FKN system because nuclear translocation of p65 took place 1 h after LPS stimulation in our experiment. Our results indicated that the p65 subunit was once translocated into the nucleus, but in complex with PPAR-γ was rapidly exported. We are not the first to describe the function of PPAR-γ in regulating inflammatory responses. When intestinal epithelial cells were treated with a strain of commensal bacteria, *Bacteroides thetaiotaomicron*, PPAR-γ underwent nucleocytoplasmic redistribution in complex with p65, which ultimately caused the attenuation of IL-8 expression induced by pathogenic *Salmonella enteritidis* (37). The role of PPAR-γ as an anti-inflammatory factor is well known; activation of PPAR-γ inhibited the expression of various cytokines in monocytes and macrophages, principally by preventing the activation of NF-κB; however, its mechanism of action is not clear (38, 39, 41). An endogenous ligand of PPAR-γ, 15d-PGJ2, a metabolite from PGD_2 (36), exerts a strong anti-inflammatory effect on macrophages. In our experiment, the effect of exogenous 15d-PGJ2 on NF-κB activation and cytokine production was very similar to that of FKN, especially at 10 μM. Since induction of 15d-PGJ2 was observed after FKN treatment, it is likely that up-regulation of 15d-PGJ2 elicited the anti-inflammatory effect in our experimental system. It was initially reported that 15d-PGJ2 affected NF-κB activation in a PPAR-γ-dependent manner (39); however, a PPAR-γ-independent pathway was also reported later (42–45). Based on the results that cellular 15d-PGJ2 was up-regulated rapidly after pretreatment with FKN and remained up-regulated for 12 h and that expression of PPAR-γ mRNA was enhanced by exogenous 15d-PGJ2 in macrophages, FKN most probably increased the level of 15d-PGJ2 first, followed by up-regulation of PPAR-γ, which

resulted in the modulation of NF-κB activation. Indeed, our experiment using PPAR-γ siRNA clearly showed that the anti-inflammatory effect of FKN depends on the presence of PPAR-γ, although we think it is still possible that FKN-induced 15d-PGJ2 or other unknown anti-inflammatory signaling pathways, independent of PPAR-γ, may directly affect expression of TLR4-MD-2 and phosphorylation of ERK1/2.

It is notable that the anti-inflammatory effect of FKN was seen when cells were pretreated with FKN at a concentration of 0.03 nM but not at 3 nM. We clearly observed a dose-dependent difference in every assay of signaling systems, such as ERK1/2 phosphorylation, complex formation of NF-κB p65 and PPAR-γ, early export of p65 from nuclei, induction of PPAR-γ mRNA, as well as up-regulation of 15d-PGJ2; all supported inhibition of TNF-α secretion by 0.03 nM but not 3 nM FKN. We could only partially clarify the mechanisms of the anti-inflammatory effect specific to this concentration of FKN. Since chemotaxis was fully triggered at 0.03 nM FKN, this concentration of FKN was sufficient to transduce classical signaling via CX3CR1. It also indicated the probability that 3 nM FKN induced additional signaling pathways, and our result demonstrated that IL-23 counteracts the anti-inflammatory effect of FKN. We assumed that this duality might be caused by differential rates of occupancy and dimerization of CX3CR1. It is possible that the proinflammatory action of FKN may depend partially on the induction of IL-23, which would be up-regulated in the cells exposed to a higher than physiological concentration of FKN. It has been shown that IL-23 is a potent activator of macrophages that enhances TNF-α expression (46) and transgenic expression of IL-23 p19 induces multiorgan inflammation (47); however, its regulatory role in mucosal inflammation is either proinflammatory (48) or anti-inflammatory (49) according to the disease models used. Such dose-dependent dual effects of FKN were not described in microglia, in which FKN was capable of attenuating LPS-induced TNF-α secretion in a dose-dependent manner (17). Differences in surface expression of LPS receptors, such as low CD14 in microglia (50), might cause this cell-specific effect. A detailed mechanism of interaction between IL-23 and FKN in macrophages is now under investigation in our laboratory. The reason why FKN has these specific effects at certain concentrations may lie in the unrevealed general mechanism of chemotaxis. Chemotaxis occurs when cells recognize a "concentration gradient" and move toward the area of higher concentration; however, the sensor mechanism for the concentration gradient is largely unknown. To determine the direction of chemotaxis, a single cell may have sensors for both low and high concentrations of ligands that mediate different signals in a three-dimensional intracellular mapping system. Our finding of dose-dependent, differential effects through CX3CR1 might represent the nature of chemokine receptors. With respect to physiological relevance, it is reasonable that cells respond in a distinct manner in the milieu of low and high concentrations of chemokine. For example, macrophages in the intestine at steady state exposed to a relatively low physiological level of FKN acquired hyporesponsiveness to LPS, which prevented an excessive inflammatory response to commensal flora. When inflammation occurs and higher concentrations of FKN and additional inflammatory cytokines are produced, newly recruited inflammatory macrophages have the potential to fully respond to produce TNF-α as an immune defense mechanism. According to previous reports, concentrations of FKN in the plasma of healthy humans were <0.03 nM (1 ng/ml) and approached 1 nM (30 ng/ml) in the plasma of patients with inflammatory airway disease (51). Thus, this study used both low and high concentrations of FKN, which may approximate those of steady-state and inflammatory situations, respectively.

Our results showed the anti-inflammatory effect of FKN, which is constitutively expressed in the colon where a high level of PPAR-γ is also expressed (52). The presence of soluble factors is known to suppress the inflammatory reaction of macrophages (32). We propose that the physiological concentration of FKN may be one such factor that maintains immune homeostasis in the intestine.

Acknowledgments

We thank Drs. Sachiko Akashi and Kensuke Miyake at Tokyo University for providing us with mAb SA15-21.

Disclosures

The authors have no financial conflict of interest.

References

1. Bazan, J. F., K. B. Bacon, G. Hardiman, W. Wang, K. Soo, D. Rossi, D. R. Greaves, A. Zlotnik, and T. J. Schall. 1997. A new class of membrane-bound chemokine with a CX3C motif. *Nature* 385: 640–644.
2. Garton, K. J., P. J. Gough, C. P. Blobel, G. Murphy, D. R. Greaves, P. J. Dempsey, and E. W. Raines. 2001. Tumor necrosis factor-α-converting enzyme (ADAM17) mediates the cleavage and shedding of fractalkine (CX3CL1). *J. Biol. Chem.* 276: 37993–38001.
3. Tsou, C. L., C. A. Haskell, and I. F. Charo. 2001. Tumor necrosis factor-α-converting enzyme mediates the inducible cleavage of fractalkine. *J. Biol. Chem.* 276: 44622–44626.
4. Fraticelli, P., M. Sironi, G. Bianchi, D. D'Ambrosio, C. Albanesi, A. Stoppacciaro, M. Chieppa, P. Allavena, L. Ruco, G. Girolomoni, et al. 2001. Fractalkine (CX3CL1) as an amplification circuit of polarized Th1 responses. *J. Clin. Invest.* 107: 1173–1181.
5. Imaizumi, T., H. Yoshida, and K. Satoh. 2004. Regulation of CX3CL1/fractalkine expression in endothelial cells. *J. Atheroscler. Thromb.* 11: 15–21.
6. Fujimoto, K., T. Imaizumi, H. Yoshida, S. Takanashi, K. Okumura, and K. Satoh. 2001. Interferon-γ stimulates fractalkine expression in human bronchial epithelial cells and regulates mononuclear cell adherence. *Am. J. Respir. Cell Mol. Biol.* 25: 233–238.
7. Umehara, H., E. T. Bloom, T. Okazaki, Y. Nagano, O. Yoshie, and T. Imai. 2004. Fractalkine in vascular biology: from basic research to clinical disease. *Arterioscler. Thromb. Vasc. Biol.* 24: 34–40.
8. Fong, A. M., L. A. Robinson, D. A. Steeber, T. F. Tedder, O. Yoshie, T. Imai, and D. D. Patel. 1998. Fractalkine and CX3CR1 mediate a novel mechanism of leukocyte capture, firm adhesion, and activation under physiologic flow. *J. Exp. Med.* 188: 1413–1419.
9. Imai, T., K. Hieshima, C. Haskell, M. Baba, M. Nagira, M. Nishimura, M. Kakizaki, S. Takagi, H. Nomiyama, T. J. Schall, and O. Yoshie. 1997. Identification and molecular characterization of fractalkine receptor CX3CR1, which mediates both leukocyte migration and adhesion. *Cell* 91: 521–530.
10. Combadiere, C., J. Gao, H. L. Tiffany, and P. M. Murphy. 1998. Gene cloning, RNA distribution, and functional expression of mCX3CR1, a mouse chemotactic receptor for the CX3C chemokine fractalkine. *Biochem. Biophys. Res. Commun.* 253: 728–732.
11. Ancuta, P., R. Rao, A. Moses, A. Mehle, S. K. Shaw, F. W. Luscinskas, and D. Gabuzda. 2003. Fractalkine preferentially mediates arrest and migration of $CD16^+$ monocytes. *J. Exp. Med.* 197: 1701–1707.
12. Nanki, T., T. Imai, K. Nagasaka, Y. Urasaki, Y. Nonomura, K. Taniguchi, K. Hayashida, J. Hasegawa, O. Yoshie, and N. Miyasaka. 2002. Migration of CX3CR1-positive T cells producing type 1 cytokines and cytotoxic molecules into the synovium of patients with rheumatoid arthritis. *Arthritis Rheum.* 46: 2878–2883.
13. Nishimura, M., H. Umehara, T. Nakayama, O. Yoneda, K. Hieshima, M. Kakizaki, N. Dohmae, O. Yoshie, and T. Imai. 2002. Dual functions of fractalkine/CX3C ligand 1 in trafficking of perforin$^+$/granzyme B^+ cytotoxic effector lymphocytes that are defined by CX3CR1 expression. *J. Immunol.* 168: 6173–6180.
14. Papadopoulos, E. J., D. J. Fitzhugh, C. Tkaczyk, A. M. Gilfillan, C. Sassetti, D. D. Metcalfe, and S. T. Hwang. 2000. Mast cells migrate, but do not degranulate, in response to fractalkine, a membrane-bound chemokine expressed constitutively in diverse cells of the skin. *Eur. J. Immunol.* 30: 2355–2361.
15. Hatori, K., A. Nagai, R. Heisel, J. K. Ryu, and S. U. Kim. 2002. Fractalkine and fractalkine receptors in human neurons and glial cells. *J. Neurosci. Res.* 69: 418–426.
16. Maciejewski-Lenoir, D., S. Chen, L. Feng, R. Maki, and K. B. Bacon. 1999. Characterization of fractalkine in rat brain cells: migratory and activation signals for CX3CR-1-expressing microglia. *J. Immunol.* 163: 1628–1635.
17. Mizuno, T., J. Kawanokuchi, K. Numata, and A. Suzumura. 2003. Production and neuroprotective functions of fractalkine in the central nervous system. *Brain Res.* 979: 65–70.
18. Volin, M. V., J. M. Woods, M. A. Amin, M. A. Connors, L. A. Harlow, and A. E. Koch. 2001. Fractalkine: a novel angiogenic chemokine in rheumatoid arthritis. *Am. J. Pathol.* 159: 1521–1530.
19. Muehlhoefer, A., L. J. Saubermann, X. Gu, K. Luedtke-Heckenkamp, R. Xavier, R. S. Blumberg, D. K. Podolsky, R. P. MacDermott, and H. C. Reinecker. 2000.

Fractalkine is an epithelial and endothelial cell-derived chemoattractant for intraepithelial lymphocytes in the small intestinal mucosa. *J. Immunol.* 164: 3368–3376.
20. Combadiere, C., S. Potteaux, J. L. Gao, B. Esposito, S. Casanova, E. J. Lee, P. Debre, A. Tedgui, P. M. Murphy, and Z. Mallat. 2003. Decreased atherosclerotic lesion formation in CX3CR1/apolipoprotein E double knockout mice. *Circulation* 107: 1009–1016.
21. Raychaudhuri, S. P., W. Y. Jiang, and E. M. Farber. 2001. Cellular localization of fractalkine at sites of inflammation: antigen-presenting cells in psoriasis express high levels of fractalkine. *Br. J. Dermatol.* 144: 1105–1113.
22. Suzuki, F., T. Nanki, T. Imai, H. Kikuchi, S. Hirohata, H. Kohsaka, and N. Miyasaka. 2005. Inhibition of CX3CL1 (fractalkine) improves experimental autoimmune myositis in SJL/J mice. *J. Immunol.* 175: 6987–6996.
23. Cockwell, P., S. J. Chakravorty, J. Girdlestone, and C. O. Savage. 2002. Fractalkine expression in human renal inflammation. *J. Pathol.* 196: 85–90.
24. Boehme, S. A., F. M. Lio, D. Maciejewski-Lenoir, K. B. Bacon, and P. J. Conlon. 2000. The chemokine fractalkine inhibits Fas-mediated cell death of brain microglia. *J. Immunol.* 165: 397–403.
25. Cook, D. N., S. C. Chen, L. M. Sullivan, D. J. Manfra, M. T. Wiekowski, D. M. Prosser, G. Vassileva, and S. A. Lira. 2001. Generation and analysis of mice lacking the chemokine fractalkine. *Mol. Cell. Biol.* 21: 3159–3165.
26. Geissmann, F., S. Jung, and D. R. Littman. 2003. Blood monocytes consist of two principal subsets with distinct migratory properties. *Immunity* 19: 71–82.
27. Niess, J. H., S. Brand, X. Gu, L. Landsman, S. Jung, B. A. McCormick, J. M. Vyas, M. Boes, H. L. Ploegh, J. G. Fox, D. R. Littman, and H. C. Reinecker. 2005. CX3CR1-mediated dendritic cell access to the intestinal lumen and bacterial clearance. *Science* 307: 254–258.
28. Fogg, D. K., C. Sibon, C. Miled, S. Jung, P. Aucouturier, D. R. Littman, A. Cumano, and F. Geissmann. 2006. A clonogenic bone marrow progenitor specific for macrophages and dendritic cells. *Science* 311: 83–87.
29. Yrlid, U., C. D. Jenkins, and G. G. MacPherson. 2006. Relationships between distinct blood monocyte subsets and migrating intestinal lymph dendritic cells in vivo under steady-state conditions. *J. Immunol.* 176: 4155–4162.
30. Lucas, A. D., N. Chadwick, B. F. Warren, D. P. Jewell, S. Gordon, F. Powrie, and D. R. Greaves. 2001. The transmembrane form of the CX3CL1 chemokine fractalkine is expressed predominantly by epithelial cells in vivo. *Am. J. Pathol.* 158: 855–866.
31. Hirotani, T., P. Y. Lee, H. Kuwata, M. Yamamoto, M. Matsumoto, I. Kawase, S. Akira, and K. Takeda. 2005. The nuclear IκB protein IκBNS selectively inhibits lipopolysaccharide-induced IL-6 production in macrophages of the colonic lamina propria. *J. Immunol.* 174: 3650–3657.
32. Smythies, L. E., M. Sellers, R. H. Clements, M. Mosteller-Barnum, G. Meng, W. H. Benjamin, J. M. Orenstein, and P. D. Smith. 2005. Human intestinal macrophages display profound inflammatory anergy despite avid phagocytic and bacteriocidal activity. *J. Clin. Invest.* 115: 66–75.
33. Shirai, Y., M. Hashimoto, R. Kato, Y. I. Kawamura, T. Kirikae, H. Yano, J. Takashima, Y. Kirihara, Y. Saito, M. A. Fujino, and T. Dohi. 2004. Lipopolysaccharide induces CD25-positive, IL-10-producing lymphocytes without secretion of proinflammatory cytokines in the human colon: low MD-2 mRNA expression in colonic macrophages. *J. Clin. Immunol.* 24: 42–52.
34. Zujovic, V., J. Benavides, X. Vige, C. Carter, and V. Taupin. 2000. Fractalkine modulates TNF-α secretion and neurotoxicity induced by microglial activation. *Glia* 29: 305–315.
35. Zujovic, V., N. Schussler, D. Jourdain, D. Duverger, and V. Taupin. 2001. In vivo neutralization of endogenous brain fractalkine increases hippocampal TNFα and 8-isoprostane production induced by intracerebroventricular injection of LPS. *J. Neuroimmunol.* 115: 135–143.
36. Shibata, T., M. Kondo, T. Osawa, N. Shibata, M. Kobayashi, and K. Uchida. 2002. 15-deoxy-Δ 12,14-prostaglandin J2: a prostaglandin D_2 metabolite generated during inflammatory processes. *J. Biol. Chem.* 277: 10459–10466.
37. Kelly, D., J. I. Campbell, T. P. King, G. Grant, E. A. Jansson, A. G. Coutts, S. Pettersson, and S. Conway. 2004. Commensal anaerobic gut bacteria attenuate inflammation by regulating nuclear-cytoplasmic shuttling of PPAR-γ and RelA. *Nat. Immunol.* 5: 104–112.
38. Jiang, C., A. T. Ting, and B. Seed. 1998. PPAR-γ agonists inhibit production of monocyte inflammatory cytokines. *Nature* 391: 82–86.
39. Ricote, M., A. C. Li, T. M. Willson, C. J. Kelly, and C. K. Glass. 1998. The peroxisome proliferator-activated receptor-γ is a negative regulator of macrophage activation. *Nature* 391: 79–82.
40. Abreu, M. T., P. Vora, E. Faure, L. S. Thomas, E. T. Arnold, and M. Arditi. 2001. Decreased expression of toll-like receptor-4 and MD-2 correlates with intestinal epithelial cell protection against dysregulated proinflammatory gene expression in response to bacterial lipopolysaccharide. *J. Immunol.* 167: 1609–1616.
41. Glass, C. K., and S. Ogawa. 2006. Combinatorial roles of nuclear receptors in inflammation and immunity. *Nat. Rev. Immunol.* 6: 44–55.
42. Straus, D. S., G. Pascual, M. Li, J. S. Welch, M. Ricote, C. H. Hsiang, L. L. Sengchanthalangsy, G. Ghosh, and C. K. Glass. 2000. 15-deoxy-Δ12,14-prostaglandin J2 inhibits multiple steps in the NF-κB signaling pathway. *Proc. Natl. Acad. Sci. USA* 97: 4844–4849.
43. Rossi, A., P. Kapahi, G. Natoli, T. Takahashi, Y. Chen, M. Karin, and M. G. Santoro. 2000. Anti-inflammatory cyclopentenone prostaglandins are direct inhibitors of IκB kinase. *Nature* 403: 103–108.
44. Thieringer, R., J. E. Fenyk-Melody, C. B. Le Grand, B. A. Shelton, P. A. Detmers, E. P. Somers, L. Carbin, D. E. Moller, S. D. Wright, and J. Berger. 2000. Activation of peroxisome proliferator-activated receptor γ does not inhibit IL-6 or TNF-α responses of macrophages to lipopolysaccharide in vitro or in vivo. *J. Immunol.* 164: 1046–1054.
45. Giri, S., R. Rattan, A. K. Singh, and I. Singh. 2004. The 15-deoxy-Δ12,14-prostaglandin J2 inhibits the inflammatory response in primary rat astrocytes via down-regulating multiple steps in phosphatidylinositol 3-kinase-Akt-NF-κB-p300 pathway independent of peroxisome proliferator-activated receptor γ. *J. Immunol.* 173: 5196–5208.
46. Cua, D. J., J. Sherlock, Y. Chen, C. A. Murphy, B. Joyce, B. Seymour, L. Lucian, W. To, S. Kwan, T. Churakova, et al. 2003. Interleukin-23 rather than interleukin-12 is the critical cytokine for autoimmune inflammation of the brain. *Nature* 421: 744–748.
47. Wiekowski, M. T., M. W. Leach, E. W. Evans, L. Sullivan, S. C. Chen, G. Vassileva, J. F. Bazan, D. M. Gorman, R. A. Kastelein, S. Narula, and S. A. Lira. 2001. Ubiquitous transgenic expression of the IL-23 subunit p19 induces multiorgan inflammation, runting, infertility, and premature death. *J. Immunol.* 166: 7563–7570.
48. Uhlig, H. H., B. S. McKenzie, S. Hue, C. Thompson, B. Joyce-Shaikh, R. Stepankova, N. Robinson, S. Buonocore, H. Tlaskalova-Hogenova, D. J. Cua, and F. Powrie. 2006. Differential activity of IL-12 and IL-23 in mucosal and systemic innate immune pathology. *Immunity* 25: 309–318.
49. Becker, C., H. Dornhoff, C. Neufert, M. C. Fantini, S. Wirtz, S. Huebner, A. Nikolaev, H. A. Lehr, A. J. Murphy, D. M. Valenzuela, et al. 2006. Cutting edge: IL-23 cross-regulates IL-12 production in T cell-dependent experimental colitis. *J. Immunol.* 177: 2760–2764.
50. Guillemin, G. J., and B. J. Brew. 2004. Microglia, macrophages, perivascular macrophages, and pericytes: a review of function and identification. *J. Leukocyte Biol.* 75: 388–397.
51. Ruth, J. H., M. V. Volin, G. K. Haines, III, D. C. Woodruff, K. J. Katschke, Jr., J. M. Woods, C. C. Park, J. C. Morel, and A. E. Koch. 2001. Fractalkine, a novel chemokine in rheumatoid arthritis and in rat adjuvant-induced arthritis. *Arthritis Rheum.* 44: 1568–1581.
52. Mansen, A., H. Guardiola-Diaz, J. Rafter, C. Branting, and J. A. Gustafsson. 1996. Expression of the peroxisome proliferator-activated receptor (PPAR) in the mouse colonic mucosa. *Biochem. Biophys. Res. Commun.* 222: 844–851.

Gasp, a Grb2-associating protein, is critical for positive selection of thymocytes

Michael S. Patrick[a,b,1], Hiroyo Oda[a,1], Kunihiro Hayakawa[a], Yoshinori Sato[a], Koji Eshima[c], Teruo Kirikae[d], Shun-ichiro Iemura[e], Mutsunori Shirai[b], Takaya Abe[f], Tohru Natsume[e], Takehiko Sasazuki[g], and Harumi Suzuki[a,2]

Departments of [a]Pathology and [d]Infectious Diseases, International Medical Center of Japan, 1-21-1 Toyama, Shinjuku, Tokyo 162-8655 Japan; [b]Department of Microbiology, Yamaguchi University School of Medicine, 1-1-1 Minami-Kogushi, Ube, Yamaguchi 755-8505 Japan; [c]Department of Immunology, Kitasato University School of Medicine, 1-15-1 Kitasato, Sagamihara, Kanagawa 228-8555 Japan; [e]National Institute of Advanced Industrial Science and Technology, Biological Information Research Center, 2-42 Aomi, Kohtoh-ku, Tokyo 135-0064 Japan; [f]Laboratory for Animal Resources and Genetic Engineering, Center for Developmental Biology, RIKEN, 2-2-3 Minatojima Minami, Chuou-ku, Kobe 65-0047 Japan; and [g]International Medical Center of Japan, 1-21-1 Toyama, Shinjuku, Tokyo 162-8655, Japan

Communicated by Tadamitsu Kishimoto, Osaka University, Osaka, Japan, July 31, 2009 (received for review June 11, 2009)

T cells develop in the thymus through positive and negative selection, which are responsible for shaping the T cell receptor (TCR) repertoire. To elucidate the molecular mechanisms involved in selection remains an area of intense interest. Here, we identified and characterized a gene product Gasp (Grb2-associating protein, also called Themis) that is critically required for positive selection. Gasp is a cytosolic protein with no known functional motifs that is expressed only in T cells, especially immature CD4/CD8 double positive (DP) thymocytes. In the absence of Gasp, differentiation of both CD4 and CD8 single positive cells in the thymus was severely inhibited, whereas all other TCR-induced events such as β-selection, negative selection, peripheral activation, and homeostatic proliferation were unaffected. We found that Gasp constitutively associates with Grb2 via its N-terminal Src homology 3 domain, suggesting that Gasp acts as a thymocyte-specific adaptor for Grb2 or regulates Ras signaling in DP thymocytes. Collectively, we have described a gene called Gasp that is critical for positive selection.

differentiation | signal transduction | T cell receptor | thymus

Development of conventional T cell receptor (TCR)-αβ T cells in the thymus requires multiple stages defined by the expression pattern of CD4 and CD8 coreceptor molecules. The most immature $CD4^-CD8^-$ [double negative (DN)] thymocytes differentiate to the $CD4^+CD8^+$ [double positive (DP)] stage through the first selection process called β-selection (pre-TCR selection). These DP thymocytes are subjected to both positive and negative selection to become either class II MHC-restricted helper $CD4^+CD8^-$ [CD4-single positive (CD4-SP)] or class I MHC-restricted cytotoxic $CD4^-CD8^+$ (CD8-SP) cells (1). After receiving positive selection signals, DP thymocytes go through an intermediate $CD4^+CD8^{lo}$ stage, irrespective of their lineage decision (2). The fate of individual DP thymocytes is determined by the strength of affinity and longevity of interaction between their TCR and peptide:MHC ligand (3). Although it is known that strong TCR/ligand interaction leads to negative selection and weak association results in positive selection (4), how this quantitative difference of TCR interaction can be converted to the qualitative difference is not known. Therefore, it is important to investigate the difference in molecular mechanisms of positive and negative selection.

One of the widely accepted models for explaining the difference between positive and negative selection is differential MAPK activation (5). Initially, differential requirements for ERK in positive selection and JNK/p38 in negative selection were focused on (6). The guanine nucleotide exchange factor (GEF) Sos has dual activity for Ras and Rac, therefore it can activate both the ERK and JNK/p38 pathways. Recently, RasGRP, which is another GEF for Ras, was shown to be critical for positive but not negative selection (7). Furthermore, mice heterozygous for Grb2, which constitutively associates with Sos, showed inefficient JNK/p38 activation, but normal ERK activation (8). From these results, positive selection signals were thought to induce the RasGRP/Ras/ERK pathway, and negative selection signals were thought to induce the Grb2-Sos/Rac/JNK p38 pathway. The model that activation through RasGRP results in weak sustained ERK activation to induce positive selection, whereas activation through Sos induces strong temporary ERK activation leading to negative selection is still widely accepted (9). Recently, Daniels et al. (10) elegantly showed that positive selection signals induced subcellular compartmentalization of RasGRP/Ras/ERK to the Golgi membrane, whereas negative selection signals induced localization of Grb2-Sos/Ras/ERK to the plasma membrane. Furthermore, positive selector-induced ERK activation lasted longer in Golgi than in the plasma membrane. Therefore, subcellular compartmentalization of Ras-GEF and Ras upon TCR stimulation is now widely accepted to be the branch point of positive and negative selection (11).

To find novel genes involved in the positive selection of thymocytes, we tried to isolate unknown genes whose expression is highly restricted to the thymus, the site where selection takes place. We used EST databases and performed in silico cloning, the strategy successfully used for isolating various novel tissue or cell type-specific genes. We selected several "thymus-specific genes" by our own computer algorithm based on their thymus-restricted expression. Among these thymus-specific genes, we focused on one gene E430004N04Rik (GeneID 210757), mainly because of its exclusive expression in immature DP thymocytes. Because we found that this protein constitutively associates with Grb2, we called the gene Gasp (Grb2-associating protein). Gasp contains no known protein motifs or homology domain and has no known function, although it has well conserved orthologs in multiple vertebrates from fish to human. To elucidate the function of Gasp, we established *Gasp*-deficient mice and found that the gene is critical for positive selection but not for other TCR-mediated signaling events.

Results

Expression of Gasp Protein. To identify novel genes specifically expressed in the thymus, we used information from the National Center for Biotechnology Information Unigene database of expressed sequence tags (ESTs). Each Unigene cluster contains information about the number of EST clones from a tissue source. We searched Unigene clusters based on the proportion of clones derived from thymus and total number of clones from the thymus. Finally, we selected five genes as thymus-specific genes. The gene Gasp (E430004N04Rik, Themis, Tsepa) was one of these thymus-specific genes. We first examined the expression of Gasp in various

Author contributions: T.S. and H.S. designed research; M.S.P., H.O., K.H., Y.S., K.E., S.-i.I., M.S., and T.N. performed research; T.K. and T.A. contributed new reagents/analytic tools; M.S.P., H.O., K.E., S.-i.I., T.N., and H.S. analyzed data; and M.S.P. and H.S. wrote the paper.

The authors declare no conflict of interest.

[1]M.S.P. and H.O. contributed equally to this work.

[2]To whom correspondence should be addressed. E-mail: hsuzuki@ri.imcj.go.jp,.

This article contains supporting information online at www.pnas.org/cgi/content/full/0908593106/DCSupplemental.

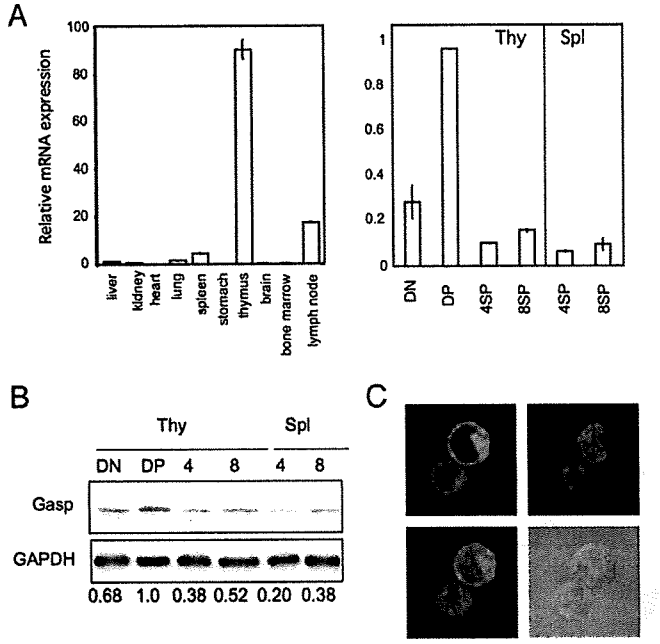

Fig. 1. Thymus-specific expression of Gasp. (*A*) Expression of Gasp mRNA was analyzed by real-time PCR from C57BL/6 mouse tissues and cells. RNA expression was normalized relative to β-actin. Error bars are the SD (n = 2 and 3). (*B*) Expression of Gasp protein in sorted thymic or splenic T cell subpopulations. Results are representative of two independent experiments. (*C*) Representative micrograph showing subcellular localization of Gasp. GFP-fused Gasp was exogenously introduced in DPK cell line (green) and costained with DAPI (blue). (Magnification: ×1,000.)

tissues and cells. As expected, mRNA expression of Gasp is highly restricted to lymphoid organs, especially in the thymus and T cells (Fig. 1*A*). Among T cell subsets, expression is highest in DP thymocytes, and its expression decreases along with maturation. The same pattern of protein expression was confirmed by Western blot analysis using Gasp-specific antibody (Fig. 1*B*). Expression of the gene in CD8-SP cells is slightly higher than in CD4-SP cells in both the thymus and spleen. Expression of Gasp in Treg cells was lower than in conventional CD4 T cells, consistent with a previous report describing Gasp as one of the most reduced genes in Tregs by comprehensive microarray analysis (12). Transcription of Gasp was not affected upon stimulation with phorbol 12-myristate 13-acetate (PMA) and ionomycin. Analysis by confocal microscopy of exogenously introduced GFP-fusion Gasp protein (both N- and C-terminal fusion protein) in a DP thymoma line (DPK) (13) showed homogeneous distribution in cytosol and exclusion from the nucleus (Fig. 1*C*). We did not observe a change in the distribution of GFP-fusion Gasp protein upon TCR stimulation.

Gasp Is Required for Positive Selection but Not for Negative Selection and β-Selection. To elucidate the precise function of Gasp, we generated *Gasp*-deficient mice by replacing the first exon of *Gasp* with a LacZ and Neo-expressing cassette (Fig. 2*A*). Protein expression of Gasp in $Gasp^{+/+}$, $Gasp^{+/-}$, and $Gasp^{-/-}$ thymocytes is shown in Fig. 2*B*, confirming the absence of Gasp protein in the deficient mice and reduced protein expression in $Gasp^{+/-}$ thymocytes. In thymi of $Gasp^{-/-}$ mice, total cell number was not significantly altered, and proportions of DN1 through DN4 in DN cells were normal, indicating that β-selection was unaffected in the mice (Table S1). However, we observed a marked decrease of CD4-SP and CD8-SP cells in the thymus (Fig. 2*C*). The effect of Gasp on positive selection is dose-dependent, because the phenotype of $Gasp^{+/-}$ mice was intermediate to that of $Gasp^{+/+}$ and $Gasp^{-/-}$ mice. Reduction of CD4-SP cells in the thymus can be observed even in the neonate, suggesting that the defect is a relatively early event in positive selection (Fig. 2*D*). To confirm the defect in positive selection, we next examined the developmental fate of thymocytes expressing three different fixed TCRs. DP thymocytes expressing class II-MHC restricted OT-II TCR transgenic (Tg) mice on a *RAG* null background did not differentiate into CD4-SP cells at all in the absence of Gasp (Fig. 2*E Top*). The class I-specific female HY-TCR Tg (14) $RAG^{-/-}$ thymocytes and OT-I TCR Tg thymocytes did not differentiate into CD8-SP cells either (Fig. 2*E Middle* and *Bottom*). Therefore, Gasp is critically required for positive selection of both thymocytes expressing class I- and class II-restricted TCR. We extensively analyzed various surface markers (e.g., CD2, CD5, HSA, CD25, class I MHC, etc.) of each stage of thymocyte development, but we did not observe significant differences between $Gasp^{+/+}$ and $Gasp^{-/-}$ thymocytes. The only difference we found was in the expression of CCR9 and CD62L (Fig. S1). Down-regulation of CCR9 on CD4-SP cells was not observed in $Gasp^{-/-}$ thymocytes, and the expression of CD62L on $Gasp^{-/-}$ CD4-SP cells was significantly decreased (Fig. S1). Differentiation of γδ-T cells in $Gasp^{-/-}$ mice was not altered (Table S1). By hematoxylin and eosin staining of thymus sections, no significant difference was observed in cortical and medullary architecture.

Because the above data show that Gasp is crucial in positive selection, we next investigated the effect of Gasp on negative selection, the other important TCR signal-initiated event. Contrary to the defect in positive selection, Gasp deficiency does not affect negative selection as the generation of DP was not recovered in the absence of Gasp in male HY-TCR Tg background (Fig. 2*F*).

***Gasp*$^{-/-}$ T Cells Expand in Periphery.** In contrast to severe impairment of positive selection in the thymus of $Gasp^{-/-}$ mice, the reduction of mature T cells in the periphery was much milder. In particular, reduction of CD8-SP cells was less significant and thus the reduction of CD4-SP cells is always severer than that in CD8-SP cells in $Gasp^{-/-}$ mice. It is noteworthy that the proportion of CD8-SP cells was even higher in $Gasp^{-/-}$ mesenteric lymph node (mLN) and inguinal lymph node (iLN) (Fig. 3*A*) compared with wild type. Because the total numbers of lymph node and spleen cells of $Gasp^{-/-}$ mice were fewer than wild type, absolute numbers of both CD4-SP and CD8-SP cells in spleen and lymph nodes were always less than in wild-type controls (Fig. 3*B*).

The less severe phenotype in number of peripheral T cells could be explained by homeostatic expansion of differentiated T cells. Therefore, we evaluated memory/activated phenotype of peripheral cells. As shown in Fig. 3*C*, CD4-SP cells in $Gasp^{-/-}$ mice contained many more memory/activated ($CD44^{hi}$ $CD62L^{-}$) phenotype cells than wild-type controls. CD8-SP cells also express CD44 at high levels, but somehow expression of CD62L was not reduced (Fig. 3*C*). Consistent with these activated phenotypes, both CD4-SP and CD8-SP cells in $Gasp^{-/-}$ mice showed significantly increased BrdU uptake in vivo, indicating that peripheral CD4-SP and CD8-SP cells in $Gasp^{-/-}$ mice proliferate without stimulation (Fig. 3*D*). Although such proliferation could be caused by autoreactive T cells, we did not see any signs of autoimmune disease in the deficient mice. We observed very few CD8-SP cells in the periphery of female HY-TCR Tg $RAG^{-/-}$, $Gasp^{-/-}$mice. Because it was reported that homeostatic proliferation does not occur in the periphery of female HY TCR-Tg mice (15), the results also support the model that the increased number of peripheral T cells in $Gasp^{-/-}$ mice was caused by homeostatic proliferation. From these results, we conclude that positive selection of CD4-SP and CD8-SP cells are both blocked in $Gasp^{-/-}$ mice, but the number of T cells in periphery is increased by homeostatic expansion.

Normal Activation of Mature *Gasp*$^{-/-}$ T Cells. We next investigated functions of peripheral T cells. Purified splenic CD4-SP cells ($CD4^{+}$, $CD8^{-}$, and $Mac1^{-}$ cells) were stimulated with immobilized

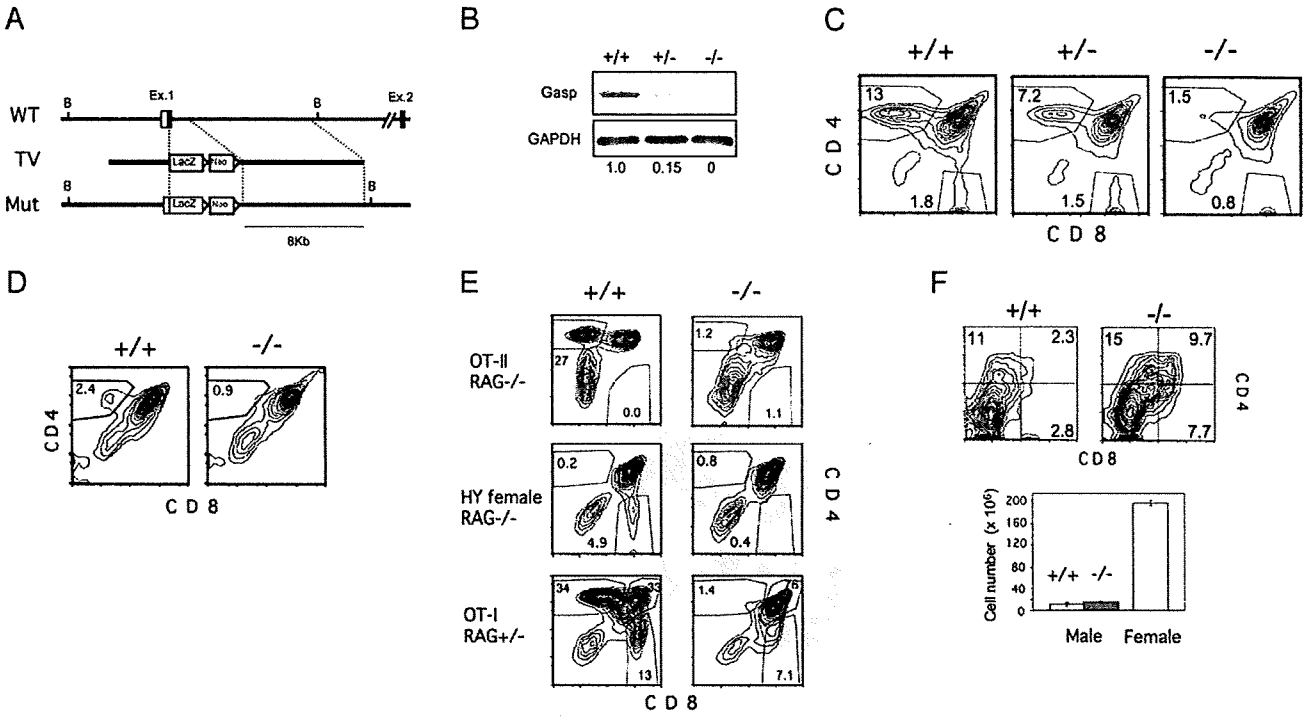

Fig. 2. Generation and analysis of *Gasp*$^{-/-}$mice. (*A*) A gene-targeting strategy was used to insert a lacZ/neo cassette into exon 1 of the Gasp gene. (*B*) Western blot analysis of DP thymocytes with anti-Gasp-specific antisera. Results are representative of two independent experiments. (*C*) CD4 and CD8 profile of *Gasp*$^{+/+}$, *Gasp*$^{+/-}$, and *Gasp*$^{-/-}$ thymocytes. (*D*) CD4 and CD8 expression of neonatal thymocytes. (*E*) CD4 and CD8 profile of thymocytes from OT-I, OT-II Tg *RAG*$^{-/-}$, and female HY Tg *RAG*$^{-/-}$mice. (*F*) CD4 and CD8 profile and number of thymocytes from male HY Tg *RAG*$^{-/-}$mice. In *C–F*, data are representative of more than three independent experiments.

anti-CD3 and CD28 antibodies in vitro, then measured for growth and IL-2 production. As shown in Fig. 4 *A* and *B*, TCR-dependent cell growth evaluated by 3-(4,5-dimethylthiazol-2-yl)-2,5-diphenyl tetrazolium bromide (MTT) assay and production of IL-2 in supernatant was comparable between *Gasp*$^{-/-}$and *Gasp*$^{+/+}$ mice. We established alloantigen (H-2^d)-specific CD4-SP and CD8-SP T cell lines from wild-type and *Gasp*$^{-/-}$splenocytes. Upon TCR stimulation, *Gasp*$^{-/-}$CD4-SP helper T cell lines produced amounts of IL-4 comparable to wild-type lines (Fig. 4*C Left*), CD8-SP CTL T cell lines produced the same amount of IFN-γ upon stimulation as wild types (Fig. 4*C Right*). We also measured CTL activity of these CD8-SP clones and found that specific killing of CD8-SP CTL clones against allogenic H-2^d MHC was not changed in the absence of Gasp (Fig. 4*D*). From these results, we conclude that activation of mature T cells does not require Gasp.

Phenotypes of *Gasp*$^{-/-}$ Thymocytes. We noticed that the phenotype of *Gasp*$^{-/-}$ mice was quite similar to *thid* (LEC) mutant rat (16). Those reports showed reduced numbers of CD4-SP cells, but not CD8-SP cells in lymph nodes (16), and lower expression of CD62L in CD4-SP cells (17), which are exactly the same phenotypes as *Gasp*$^{-/-}$mice. The responsible gene for *thid* mutation was recently reported as *PTPRK* (protein tyrosine phosphatase receptor K) (18, 19), and the gene is only 100 Kb apart from the *Gasp* gene locus. To exclude the possibility that the disturbance of expression of the adjacent *PTPRK* gene was responsible for the phenotype of *Gasp*$^{-/-}$ mice, we analyzed expression of PTPRK mRNA in *Gasp*$^{-/-}$ thymocytes by real-time RT-PCR analysis. The expression of PTPRK is not reduced but rather increased in *Gasp*$^{-/-}$thymocytes (Fig. 5*A*). Therefore, the phenotype of *Gasp*$^{-/-}$ mice is likely independent of PTPRK.

We next performed bone marrow chimera experiments to investigate whether the developmental defect in the thymus was caused by an intrinsic thymocyte defect or a defect in the thymic microenvironment. As shown in Fig. 5*B*, thymocytes from wild-type bone marrow developed normally in irradiated *Gasp*$^{-/-}$ mice, whereas wild-type mice reconstituted with *Gasp*$^{-/-}$ bone marrow showed almost identical phenotypes as *Gasp*$^{-/-}$ mice. Therefore, the defect is thymocyte intrinsic, which is consistent with the specific expression of Gasp in thymocytes (Fig. 1*A*).

We next analyzed the expression of TCR on thymocytes. Although TCR-β expression on CD4-SP cells in the thymus is consistently lower than wild type, expression of TCR on preselected DP and peripheral mature T cells (Fig. S2 *A* and *B*) were comparable to the wild type. Expression of TCR on DP thymocytes of TCR-Tg mice was also not significantly changed (Fig. S2*C*). Furthermore, spontaneous and TCR-induced cell death evaluated by AnnexinV staining was not significantly different in the absence of Gasp (Fig. S3).

Signal Transduction in *Gasp*$^{-/-}$ DP Cells. We next focused on the DP stage when positive selection takes place. We observed a significant reduction in the earliest postselected DP (CD69^{hi} TCR^{hi} DP) in *Gasp*$^{-/-}$mice (Fig. 5*C*), suggesting that the defect lies in a relatively early phase of the selection process. We next investigated TCR-stimulated signal transduction of DP thymocytes. Stimulation with plate-coated anti-CD3 plus CD28 antibody successfully induced CD69 up-regulation on *Gasp*$^{-/-}$DP thymocytes (Fig. 5*D*), indicating that the signaling pathway leading to CD69 transcription was not affected. In accordance with that, anti-CD3 mAb induced Ca^{2+} influx in DP thymocytes was not significantly disturbed (Fig. 5*E*). Furthermore, anti-CD3 mAb induced phosphorylation of ERK, phospholipase C γ (PLC-γ), and SLP76, all were unaltered in *Gasp*-deficient DP thymocytes (Fig. 5*F*).

Gasp Constitutively Associates with Grb2. To figure out the function of Gasp further, we attempted to identify proteins associated with

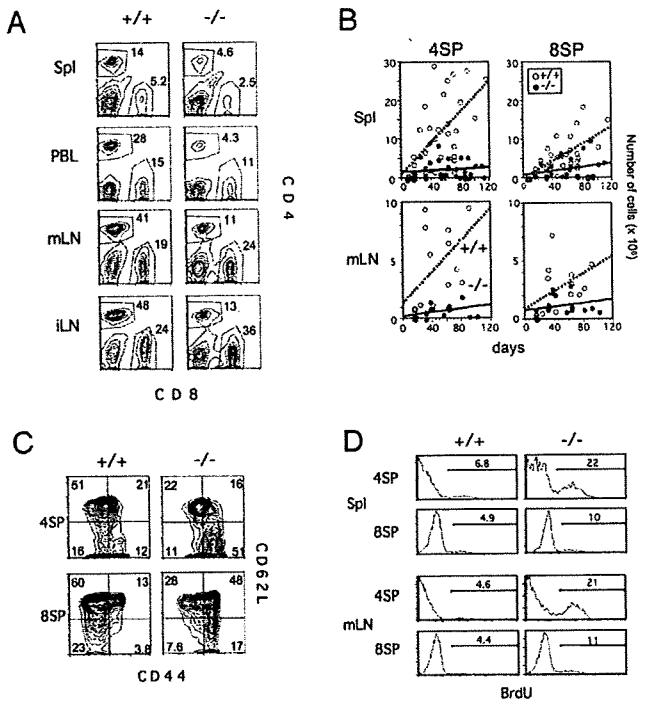

Fig. 3. Phenotype of peripheral T cells in *Gasp*$^{-/-}$mice. (*A*) CD4 and CD8 profile of the cells from spleen, peripheral blood (PBL), mLN, and iLN of *Gasp*$^{+/+}$ and *Gasp*$^{-/-}$ mice. Results are representative of more than five independent experiments. (*B*) Absolute number of CD4-SP and CD8-SP cells of Spl and mLN of *Gasp*$^{+/+}$ and *Gasp*$^{-/-}$ mice. Each dot represents individual mice at day of age. Solid (−/−) and dashed (+/+) lines show the linear regression correlation between age and absolute number of cells. (*C*) CD44 and CD62L profile of splenic CD4-SP and CD8-SP cells from *Gasp*$^{+/+}$ and *Gasp*$^{-/-}$ mice. (*D*) BrdU uptake of CD4-SP and CD8-SP cells from spleen and mLN of *Gasp*$^{+/+}$ and *Gasp*$^{-/-}$ mice. After mice were fed with BrdU for 5 days with drinking water, the cells were stained with anti-BrdU antibody. In *C* and *D*, results are representative of more than three independent experiments.

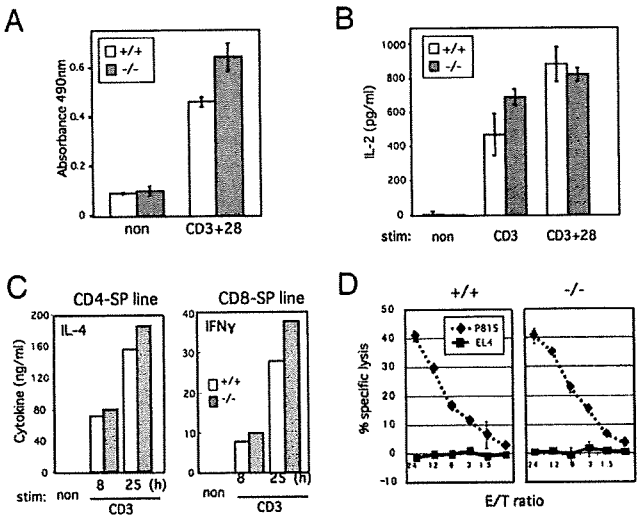

Fig. 4. Activation of peripheral CD4 and CD8 mature T cells. (*A*) MTT assay was applied for TCR-stimulated sorted splenic CD4-SP cells of *Gasp*$^{+/+}$ and *Gasp*$^{-/-}$ mice after 3 days of culture. (*B*) Primary CD4-SP T cells from *Gasp*$^{+/+}$ and *Gasp*$^{-/-}$ mice were stimulated with plate-bound anti-CD3 or CD3^{+} 28 mAb for 24 h, and IL-2 concentration in supernatants was measured by ELISA. (*C*) TCR-dependent production of IL4 and IFN-γ from cell line established from *Gasp*$^{+/+}$ and *Gasp*$^{-/-}$ splenocyte. (*D*) H-2^{d}-specific allo-CTL lines were established from splenic CD8-SP cells, and CTL assay was analyzed for CTL function by using specific (P815) and nonspecific (EL4). Results are representative of more than two independent experiments.

Gasp by using liquid chromatography-based electrospray tandem mass spectrometry (20). Human embryonic kidney cells were transfected with Flag-tagged human Gasp, and lysates from these cells were immunoprecipitated with anti-Flag antibody. Immunoprecipitated proteins were subjected to proteolysis followed by liquid chromatography-based electrospray tandem mass spectrometry. The analysis gave us several candidate Gasp-associating proteins. Among them, the most frequently detected amino acid sequences were derived from Grb2. Grb2 is an adaptor protein constitutively associated with Sos, having two Src homology 3 (SH3) domain (N and C terminus) and one SH2 domain in the middle (21). Therefore, we next performed coimmunoprecipitation experiments using Flag-tagged Gasp and myc-tagged Grb2 and their mutants. As shown in Fig. 6, myc-Grb2 could successfully pull down Flag-Gasp, and Flag-Gasp also coprecipitated myc-Grb2. Although a Grb2 mutant lacking the entire SH2 region (Grb2-ΔSH2) could associate with Gasp, an SH3 mutant (Grb2–42L/203R) in which both the N- and C-terminal SH3 domains were mutated (22) could not (Fig. 6). Because Grb2–203R in which only the C-terminal SH3 domain was mutated could associate with Gasp (Fig. 6*B*), Gasp likely associates with Grb2 via its N-terminal SH3 region, which is the same binding site for Sos (23). We noticed that Gasp contains a proline-rich sequence (^{555}PPPRPPKHP) in its C terminus. Although it is different from the consensus Grb2 SH3 domain binding sequence (PVPPPVPPR), we made a deletion mutant of this proline-rich sequence (HA-Gasp-ΔPro) and tested its interaction with Grb2. As shown in Fig. S4, we found that the association was independent of this proline-rich region. We also found Gasp was not tyrosine-phosphorylated upon TCR stimulation or PMA+ionomycin stimulation (Fig. S5), consistent with the observation that treatment with pervanadate did not augment the association of Gasp and Grb2.

Discussion

Although it is well known that both positive selection and negative selection are evoked by stimulation of TCRs of different affinities, the molecular basis of these selection processes is poorly understood. The molecules exclusively required for either selection process will give us a hint to figure out the molecular mechanism of these two selections. At present, ERK (24), Calcineurin (25), TCR-αcpm (26), and RasGRP (7) are described to be required only for positive selection but not for negative selection, whereas bim (26), MINK (27), and nur77 (28) are required only for negative selection. We have now added another gene to the list of players required for positive selection.

Gasp, which is preferentially expressed in immature DP thymocytes, has quite unique characteristics. Most of the proteins reported to be required for positive selection are involved in TCR-induced signal transduction. As a result, other TCR-related signaling events such as peripheral activation and homeostatic expansion are also affected. Unlike other positive selection-deficient mutant mice, *Gasp*$^{-/-}$ mice showed a defect only in positive selection among all of the TCR-induced signaling events. However, it should be noted that the male HY-TCR Tg system may not be appropriate for assessment of physiological negative selection because developmental arrest occurs before the DP stage (29).

In the periphery of *Gasp*$^{-/-}$ mice, the number of CD8-SP cells in lymph nodes was more than CD4-SP cells, suggesting some effect of Gasp on CD4/CD8 lineage choice. However, analysis of three independent TCR Tg mice clearly showed there is no lineage conversion nor incomplete block in positive selection of class I-restricted TCR.

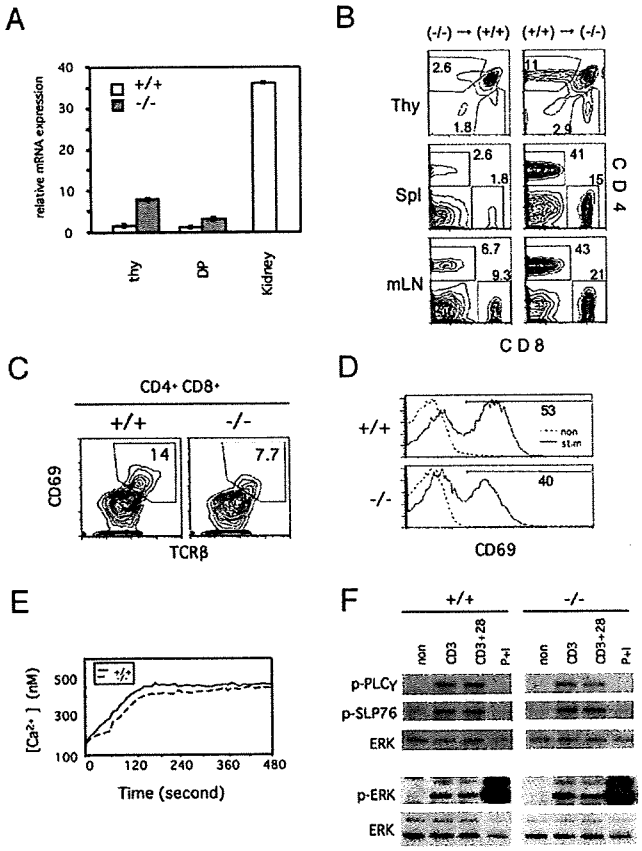

Fig. 5. Characteristics of Gasp deficiency. (*A*) Defects in *Gasp*$^{-/-}$ mice are independent of PTPRK. Expression of PTPRK mRNA in *Gasp*$^{-/-}$ thymocytes was determined by real-time RT-PCR. Error bars are the SD (n = 2 and 3). (*B*) Developmental defects in *Gasp*$^{-/-}$ mice are thymocyte intrinsic. Bone marrow cells from CD45.1 *Gasp*$^{+/+}$ mice were injected into lethally irradiated CD45.2 *Gasp*$^{-/-}$ mice or vice versa. After 2 months, cells from indicated organs were stained with CD4, 8, 45.1, and 45.2. Results are representative of more than two independent mice. (*C*) Proportion of post-selected CD69^{+} TCR^{hi} DP cells in *Gasp*$^{+/+}$ and *Gasp*$^{-/-}$ mice. Results are representative of four independent experiments. (*D*) Sorted DP thymocytes from *Gasp*$^{+/+}$ and *Gasp*$^{-/-}$mice were activated with plate-bound CD3 + 28 Ab overnight, then stained with CD69. Results are representative of more than three independent experiments. (*E*) DP cells from *Gasp*$^{-/-}$ mice were stimulated with anti-CD3 mAb followed by anti-hamster IgG, then Ca^{2+} concentration was measured by using Fura2-AM. Results are representative of three independent experiments. (*F*) DP thymocytes were activated by the indicated stimuli (2 min for anti-CD3 and 3 + 28, 5 min for PMA+Iono), then Western blotted with phosphorylated-ERK-, SLP76-, and PLCγ-specific antibody. Results are representative of more than three independent experiments.

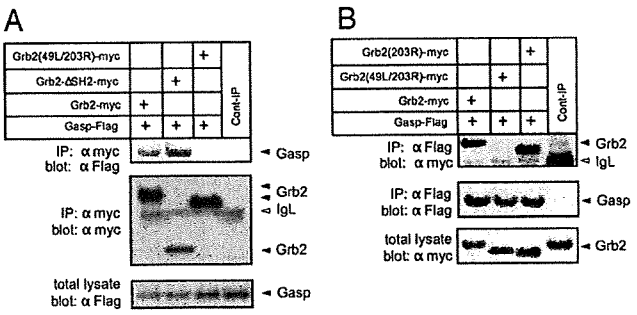

Fig. 6. Gasp associates with Grb2. (*A*) HEK293T cells were transfected with myc-tagged Grb2, SH2-deleted Grb2 (Grb2-SH2-myc), N-/C-terminal SH3 mutant (Grb2–49L/203R-myc), and Flag-tagged Gasp. Lysates were immunoprecipitated with anti-Flag mAb then blotted with the indicated Abs. (*B*) myc-Grb2, Grb2–49L/203R, C-terminal SH3 mutant (Grb2–203R-myc) ,and Flag-Gasp were transfected and immunoprecipitated with anti-myc mAb then blotted with the indicated Abs. Results are representative of more than seven independent experiments.

Reduction of CD69^{+}TCR^{hi}DP in *Gasp*$^{-/-}$mice and the disappearance of CD4^{+}CD8^{lo} post-selected cells (2) in OT-I TCR Tg thymocytes also indicate that the defect in positive selection is relatively early and affects both CD4 and CD8 lineages. We found that a large part of peripheral *Gasp*$^{-/-}$ T cells are actively proliferating without antigenic stimulation, and that is why the peripheral phenotype of *Gasp*$^{-/-}$ mice is much milder than that in the thymus. Because we do not observe any signs of autoimmune symptom in even >1-year-old *Gasp*$^{-/-}$mice, these proliferating T cells are not autoreactive, but expand by homeostatic proliferation. We always observed severer reductions in CD4-SP cells than CD8-SP cells in the periphery of *Gasp*$^{-/-}$mice. Furthermore, higher expression of CD62L in Gasp$^{-/-}$ CD8-SP cells could explain preferential migration of CD8-SP cells into lymph nodes.

Our finding that Gasp constitutively associated with Grb2 is quite intriguing and provides some possible links to hypothesize its function in positive selection, because Grb2 is an important adaptor for Sos in the TCR-mediated signal transduction pathway. According to the currently well-accepted model (5, 9–11, 30), Grb2/Sos activation is involved only in negative selection. Because Gasp could compete with Sos for binding to Grb2, existence of Gasp would likely inhibit negative selection, which does not explain the current phenotype well. However, there is no direct evidence that Sos is required for thymic selection, because Sos1 deletion is embryonic lethal (31), and Sos2-deficient mice showed no phenotype (32). Although an earlier study using Grb2$^{+/-}$ mice suggested Grb2 is involved in negative selection but not in positive selection (8), recent results from lck-Cre driven Grb2 conditional deficient mice suggests that Grb2 is required for positive selection. According to these facts, Gasp is more likely to function as an adaptor for Grb2, bringing some unknown molecule required for positive selection to the LAT signalosome complex. If Gasp functions in TCR-mediated signal transduction, it is surprising that *Gasp*$^{-/-}$ DP thymocytes did not show any defect in signal transduction induced by various dose ranges (5–0.1 μg/mL) of anti-TCR antibody. However, it is still possible that *Gasp*$^{-/-}$ thymocytes have signaling defects when stimulated by weaker signals or physiological MHC/peptide ligands.

In conclusion, we found a Grb2-associating protein that is specifically expressed in the thymus and is critical in positive selection but not in other TCR-related signal transduction events. Detailed function of the protein in positive selection should be studied further.

We would like to note that, during the review process of this article, several other groups' reports describing the same gene under the name "*Themis*" were published (33–35, 40).

Materials and Methods

Mice. *Gasp*$^{-/-}$ mice (CDB0574K: www.cdb.riken.jp/arg/mutant%20mice%20list.html) were generated as described (36, 37). The first exon of *Gasp* was targeted by homologous recombination using vector backbone DT-A/LacZ/neo with 5′ and 3′ flanking arms of 4 and 8 kbp, respectively. Neomycin-selected ES cell lines were screened by PCR, and two independent mouse lines were established. Southern blot analysis confirmed target gene deletion. The two independent mouse lines showed identical phenotypes. OT-I, OT-II, and HY mice have been described (14). All mice were housed under specific pathogen-free conditions and used in accordance with International Medical Center of Japan institutional guidelines.

Real-Time RT-PCR. Total RNA was isolated from tissues or cells by using the RNeasy kit (Qiagen). cDNA generated by SuperScript III (Invitrogen) was analyzed by using primers for the indicated gene and the Platinum SYBR Green qPCR-UDG Supermix with ROX (Invitrogen). Results were normalized to β-actin expression levels. Primer sequences for Gasp, PTPRK, and β-actin are available on request.

Immunoprecipitations and Western Blot Analysis. Transfection and immunoprecipitation were performed as described (38) with the exception of using 0.05% Nonidet P-40 lysis buffer. Antibodies for Western blot analysis were against: pPLCγ-1, ERK, and pERK (Cell Signaling) and pSLP76 (BD Biosciences). Anti-Gasp-specific rabbit antiserum was generated by injection of recombinant full-length Gasp protein. Antibodies used for immunoprecipitations were: anti-myc (9E10), anti-HA (Roche), and anti-FLAG (M2, Sigma). Horseradish peroxidase-conjugated anti-IgG secondary antibodies against rabbit, rat, and mouse (GE Healthcare) were used with Lumiglo (Cell Signaling) substrate.

Plasmids and Recombinant DNAs. Full-length murine Gasp cDNA was PCR-cloned using IMAGE clone 40130002 (OpenBiosystems) as template into pcDNA3 vector to generate Gasp-HA. To generate Gasp-ΔPro-HA, the proline-rich sequence ^{555}PPPRPPKHP of Gasp was deleted by site-directed PCR mutagenesis. A BamHI and XbaI fragment from pSVEGrb49L or pSVEGrb49L/203R (kind gifts from Robert Weinberg, Whitehead Institute, Cambridge, MA) was cloned into to pcDNA3.1 to generate Grb2(203R)-myc and Grb2(49L/203R)-myc. Grb2-myc and Grb2-ΔSH2-myc were kind gifts from Kazuo Sugamura, Tohoku University, Sendai, Japan.

Establishment of CD8$^+$ and CD4$^+$ T Cell Lines. The CD8$^+$ or CD4$^+$ T cell lines were established in vitro by stimulating splenocytes from *Gasp*$^{+/+}$ and *Gasp*$^{-/-}$ mice after depleting CD4$^+$ or CD8$^+$ cells, with BALB/c (allogeneic) splenocytes or syngeneic splenocytes in the presence of 2C11 (1 μg/mL). T cell lines were maintained by biweekly stimulations in complete DMEM supplemented with 10% prescreened FCS and 5% conditioned medium that was prepared from culture supernatant of rat splenocytes stimulated with Con A for 48 h.

Cell-Mediated Lymphocytotoxicity Assay. Graded numbers of anti-H-2^d CD8$^+$ T cells were incubated with 5,000 ^{51}Cr-labeled P815 (H-2^d mastcytoma) or EL4 (H-2^b T lymphoma) for 4 h. The supernatants were harvested with the Skatron harvesting system, and radioactivities in the supernatants were measured with a gamma counter. Assays were performed in triplicate.

Cell Stimulation Assays. CD4CD8 DP thymocytes were sorted (FACSAria II; Becton Dickinson) and stimulated with soluble or plate-bound anti-CD3 (clone 2C11) and anti-CD28 antibody each at 5 μg/mL for the indicated times. After 24 h of stimulation IL-2 production was measured in supernatant by mouse IL-2 ELISA Ready-SET-Go! (Ebioscience). Analysis of pERK used CD3 or CD3+CD28 at 5 μg/mL and goat anti-hamster (GAH) Ab at 40 μg/mL.

Ca^{2+} Mobilization Measurements. Sorted CD4CD8 DP cells were labeled with 3 μM Fura2-AM (Molecular Probes/Invitrogen) for 1 h at 37 °C. Cells were washed with ice-cold PBS and resuspended in Ringer's solution. Five million cells were surface-labeled with CD3 or CD3 + 28 at 5 μg/mL on ice for 20 min. Labeled cells were washed and warmed up for 5 min in a cuvette, then cross-linked with 40 μg/mL GAH and analyzed with a fluorescence spectrophotometer (Hitachi F-2500) for fluorescence intensity every 10 s for up to 10 min.

BrdU Administration and FACS Analysis. Mice were fed 0.8 mg/mL BrdU (Nacalai Tesque) for 5 days in drinking water. Antibodies used for staining were phycoerythrin (PE)-antiCD4 (GK1.5; Ebioscience), allophycocyanin (APC)-antiCD8 (53-6.7; Biolegend). and FITC-antiBrdu (3D4; BD Pharmingen). Cells were isolated from spleens and mLN, surface-stained for CD4-PE and CD8-APC, and stained for BrdU incorporation as described (39).

ACKNOWLEDGMENTS. We thank Meiko Fujino and Meiko Takeshita for expert technical assistance; Makoto Koyanagi, Taeko Dohi, Shigeyuki Kano, and Hiroki Aoki for technical advice; Nobukata Shinohara for support; Nobuko Saito, Yusuke Matsuoka, and Tohru Miyoshi-Akiyama for expertise in antibody production; and Shigeo Koyasu for critical reading of the manuscript. This work was supported by Grant-in-Aid for Scientific Research in Priority Areas 20060039 from the Ministry of Education, Culture, Sports, Science, and Technology of Japan.

1. Rothenberg EV, Taghon T (2005) Molecular genetics of T cell development. *Annu Rev Immunol* 23:601–649.
2. Suzuki H, Punt JA, Granger LG, Singer A (1995) Asymmetric signaling requirements for thymocyte commitment to the CD4$^+$ versus CD8$^+$ T cell lineages: A new perspective on thymic commitment and selection. *Immunity* 2:413–425.
3. Starr TK, Jameson SC, Hogquist KA (2003) Positive and negative selection of T cells. *Annu Rev Immunol* 21:139–176.
4. Germain RN (2003) Ligand-dependent regulation of T cell development and activation. *Immuol Res* 27:277–286.
5. Alberola-Ila J, Hernandez-Hoyos G (2003) The Ras/MAPK cascade and the control of positive selection. *Immunol Rev* 191:79–96.
6. Rincon M, Flavell RA, Davis RA (2000) The JNK and P38 MAP kinase signaling pathways in T cell-mediated immune responses. *Free Radical Biol Med* 28:1328–1337.
7. Dower NA, et al. (2000) RasGRP is essential for mouse thymocyte differentiation and TCR signaling. *Nat Immunol* 1:317–321.
8. Gong Q, et al. (2001) Disruption of T cell signaling networks and development by Grb2 haploid insufficiency. *Nat Immunol* 2:29–36.
9. Miosge L, Zamoyska R (2007) Signaling in T cell development: Is it all location, location, location? *Curr Opin Immunol* 19:194–199.
10. Daniels MA, et al. (2006) Thymic selection threshold defined by compartmentalization of Ras/MAPK signaling. *Nature* 444:724–729.
11. Yasuda T, Kurosaki T (2008) Regulation of lymphocyte fate by Ras/ERK signals. *Cell Cycle* 7:3634–3640.
12. Marson A, et al. (2007) Foxp3 occupancy and regulation of key target genes during T cell stimulation. *Nature* 445:931–935.
13. Kaye J, Ellenberger DL (1992) Differentiation of an immature T cell line: A model of thymic-positive selection. *Cell* 71:423–435.
14. Kisielow P, Teh HS, Bluthmann H, von Boehmer H (1988) Positive selection of antigen-specific T cells in thymus by restricting MHC molecules. *Nature* 335:730–733.
15. Park JH, et al. (2007) Coreceptor tuning: Cytokine signals transcriptionally tailor CD8 coreceptor expression to the self-specificity of the TCR. *Nat Immunol* 8:1049–1059.
16. Yamada T, et al. (1991) Inheritance of T helper immunodeficiency (thid) in LEC mutant rats. *Immunogenetics* 33:216–219.
17. Jung CG, Miyamoto T, Tsumagari T, Agui T (2001) Genetic association between low expression phenotype of CD62L (L-selectin) in peripheral CD4$^+$ T cells and the thid (T-helper immunodeficiency) phenotype in the LEC rat. *Exp Anim* 50:337–340.
18. Asano A, Tsubomatsu K, Jung CG, Sasaki N, Agui T (2007) A deletion mutation of the protein tyrosine phosphatase κ (Ptprk) gene is responsible for T-helper immunodeficiency (thid) in the LEC rat. *Mamm Genome* 18:779–786.
19. Kose H, et al. (2007) Maturational arrest of thymocyte development is caused by a deletion in the receptor-like protein tyrosine phosphatase κ gene in LEC rats. *Genomics* 89:673–677.
20. Natsume T, et al. (2002) A direct nanoflow liquid chromatography–tandem mass spectrometry system for interaction proteomics. *Anal Chem* 74:4725–4733.
21. Chardin P, Cussac D, Maignan S, Ducruix A (1995) The Grb2 adaptor. *FEBS Lett* 369:47–51.
22. Egan SE, et al. (1993) Association of Sos Ras exchange protein with Grb2 is implicated in tyrosine kinase signal transduction and transformation. *Nature* 363:45–51.
23. Cussac D, Frech M, Chardin P (1994) Binding of the Grb2 SH2 domain to phosphotyrosine motifs does not change the affinity of its SH3 domains for Sos proline-rich motifs. *EMBO J* 13:4011–4021.
24. Fischer AM, Katayama CD, Pages G, Pouyssegur J, Hedrick SM (2005) The role of erk1 and erk2 in multiple stages of T cell development. *Immunity* 23:431–443.
25. Neilson JR, Winslow MM, Hur EM, Crabtree GR (2004) Calcineurin B1 is essential for positive but not negative selection during thymocyte development. *Immunity* 20:255–266.
26. Werlen G, Hausmann B, Palmer E (2000) A motif in the αβ T cell receptor controls positive selection by modulating ERK activity. *Nature* 406:422–426.
27. McCarty N, et al. (2005) Signaling by the kinase MINK is essential in the negative selection of autoreactive thymocytes. *Nat Immunol* 6:65–72.
28. Zhou T, et al. (1996) Inhibition of Nur77/Nurr1 leads to inefficient clonal deletion of self-reactive T cells. *J Exp Med* 183:1879–1892.
29. Takahama Y, Shores EW, Singer A (1992) Negative selection of precursor thymocytes before their differentiation into CD4$^+$CD8$^+$ cells. *Science* 258:653–656.
30. McNeil LK, Starr TK, Hogquist KA (2005) A requirement for sustained ERK signaling during thymocyte positive selection in vivo. *Proc Natl Acad Sci USA* 102:13574–13579.
31. Qian X, et al. (2000) The Sos1 and Sos2 Ras-specific exchange factors: Differences in placental expression and signaling properties. *EMBO J* 19:642–654.
32. Esteban LM, et al. (2000) Ras-guanine nucleotide exchange factor sos2 is dispensable for mouse growth and development. *Mol Cell Biol* 20:6410–6413.
33. Fu G, et al. (2009) Themis controls thymocyte selection through regulation of T cell antigen receptor-mediated signaling. *Nat Immunol* 10:848–856.
34. Johnson AL, et al. (2009) Themis is a member of a new metazoan gene family and is required for the completion of thymocyte positive selection. *Nat Immunol* 10:831–839.
35. Lesourne R, et al. (2009) Themis, a T cell-specific protein important for late thymocyte development. *Nat Immunol* 10:840–847.
36. Yagi T, et al. (1993) A novel ES cell line, TT2, with high germ line-differentiating potency. *Anal Biochem* 214:70–76.
37. Murata T, et al. (2004) *ang* is a novel gene expressed in early neuroectoderm, but its null mutant exhibits no obvious phenotype. *Gene Expr Patterns* 5:171–178.
38. Oda H, et al. (2009) RhoH plays critical roles in Fcε RI-dependent signal transduction in mast cells. *J Immunol* 182:957–962.
39. Tough DF, Sprent J (1994) Turnover of naive- and memory-phenotype T cells. *J Exp Med* 179:1127–1135.
40. Kakugawa K, et al. (2009) A novel gene essential for the development of single positive thymocytes. *Mol Cell Biol* 29:5128–5135.

Immunology Letters xxx (2009) xxx–xxx

Contents lists available at ScienceDirect

Immunology Letters

journal homepage: www.elsevier.com/locate/

Rac GTPases are involved in development, survival and homeostasis of T cells

Yoshinori Sato[a], Hiroyo Oda[a], Michael S. Patrick[a], Yukari Baba[b], Ahmed A. Rus'd[b], Yoshinao Azuma[b], Takaya Abe[c], Mutsunori Shirai[b], Harumi Suzuki[a,*]

[a] Department of Pathology, Research Institute, International Medical Center of Japan, 1-21-1 Toyama, Shinjuku, Tokyo 162-8655, Japan
[b] Department of Microbiology, Yamaguchi University School of Medicine, Ube 755-8685, Japan
[c] Laboratory for Animal Resources and Genetic Engineering, Center for Developmental Biology, RIKEN Kobe, Chuou-ku, Kobe 650-0047, Japan

ARTICLE INFO

Article history:
Received 27 February 2009
Received in revised form 23 March 2009
Accepted 29 March 2009
Available online xxx

Keywords:
Rac
T cell survival and homeostasis

ABSTRACT

Rac GTPases consist of Rac1, 2 and 3, and each of them have redundant and differential functions. Rac1 is the most ubiquitously and abundantly expressed of the three and has been shown to work as a "molecular switch" in various signal transduction pathways. Although Rac1 and Rac2 are both activated by TCR ligation, little is known about the function of Rac GTPases in the development and activation of T cells. In order to investigate the precise function of Rac GTPases in T cells in vivo, we established dominant negative Rac1 transgenic (dnRac1-Tg) mice controlled by the human CD2 promoter. Total numbers of thymocytes of dnRac1-Tg mice were significantly decreased because of impaired transition from the CD4CD8 double negative stage to the CD4CD8 double positive (DP) stage. Although positive selection of CD4 single positive (SP) was not altered, positive selection of CD8-SP was slightly increased. On the contrary, the number of mature CD4-SP and CD8-SP cells in the spleen, mesenteric lymph nodes and peripheral blood was severely decreased in dnRac1-Tg mice. Proliferation of splenic CD4-SP cells upon TCR stimulation in vitro was unaltered, however, homeostatic proliferation of dnRac1-Tg splenic CD4-SP cells in lymphopenic mice was severely reduced. Finally, we found increased spontaneous apoptosis of DP thymocytes and mature T cells in dnRac1-Tg mice, possibly because of reduced phosphorylation of Akt with or without TCR stimulation. Collectively, the current results indicate that Rac GTPases are important in survival of DP thymocytes and mature T cells in vivo by regulating Akt activation.

1. Introduction

Rac belongs to the Rho family of small guanosinetriphosphatases (GTPases), and is a critical signaling regulator acting as a molecular switch in mammalian cells [1–4]. Rac consists of three independent genes; Rac1 is expressed ubiquitously, Rac2 is expressed only in hematopoietic cells, and Rac3 is expressed mainly in the brain [1–5]. Rac1 regulates various cellular functions such as cellular growth, cytoskeletal rearrangement, and apoptosis [6–8]. Rac2 is important for superoxide production, phagocytosis by neutrophils, regulation of leukocyte lineage differentiation, regulation of B cell adhesion and immunological-synapse formation [9–11]. Rac3 is relevant to later events in the development of a functional nervous system [12]. Because Rac1 deficient mice die in utero [13], a conditional knockout strategy was applied for the analysis of its function. Distinct and critical roles of Rac1 and Rac2 in growth and engraftment of hematopoietic stem cells [5,14,15] as well as in B cell development [16] were reported by using conditional knockout mice for Rac1 on a Rac2$^{-/-}$ background.

However, little is known about the function of Rac GTPases in T cell development and activation. Rac2-deficient mice showed normal T cell development in the thymus, defective Th1 differentiation caused by decreased IFN-γ production [17], perturbed chemotaxis [18], and defective T cell activation accompanied by decreased ERK activation [19]. Overexpression of constitutively active mutants of Rac1 (L61Rac1 and L61Y40CRac1) induced pre-T cell differentiation and proliferation on a RAG$^{-/-}$ background [20], and conversion of positive selection to negative selection in the thymus [21]. The results indicates that Rac1 regulates the strength of TCR-mediated signal transduction. Very recently, mice with conditional disruption of both Rac1 and Rac2 in the thymus were reported and they showed reduced development of T cell and impaired activation with increased cell death [22,23].

Although Rac1 and Rac2 are abundantly expressed in the thymus, we found that Rac3 too was weakly expressed in the thymus. Because all three Rac GTPases are expressed in the thymus, we decided to establish transgenic mice with thymocyte-specific expression of a dominant negative mutant form of Rac1

* Corresponding author. Tel.: +81 3 3232 3100; fax: +81 3 3232 3100.
E-mail address: hsuzuki@ri.imcj.go.jp (H. Suzuki).

0165-2478/$ – see front matter © 2009 Elsevier B.V. All rights reserved.
doi:10.1016/j.imlet.2009.03.014

(N17 mutation), which is known to inhibit all three Rac GTPases [24]. Overexpression of the dominant negative (dn) Rac1N17 mutant cDNA in a T cell line successfully inhibited TCR/CD28-dependent Rac signaling downstream of Vav [25,26]. In the current study, dnRac1 transgenic (Tg) mice whose expression is controlled by human CD2 promoter showed impaired β-selection in the thymus and decreased numbers of peripheral mature T cells. TCR-stimulated proliferation of dnRac1-expressing T cells in vitro was not affected, but homeostatic proliferation of mature T cells was significantly decreased. Spontaneous apoptosis as well as TCR-induced apoptosis of T cells were increased with defective phosphorylation of Akt. These results indicate that Rac GTPases are important in proliferation, survival and homeostasis of T cells.

2. Materials and methods

2.1. Generation of dominant negative Rac1 transgenic mice

Dominant negative (N17) mutant Rac1 cDNA was cloned into the CD2-VA cassette [27] and the construct was microinjected into male pronuclei of C57Bl/6 fertilized eggs to establish transgenic mouse lines (hCD2-dnRac1-LCR transgenic mice: Acc. No. CDB0448T; http://www.cdb.riken.jp/arg/mutant%20mice%20list.html). Four different transgene-expressing lines were obtained and line#22 which showed the highest expression was used in the current study. The experiments described in this study were performed in adherence to institutional ethical guidelines for animal experiments and safety guidelines for gene manipulation experiments. Approval by the Animal Use Committee of the Research Institute of International Medical Center of Japan was obtained before the start of the experiments.

2.2. FACS analysis and antibodies

Thymocytes and peripheral T cells were stained with various combinations of FITC-conjugated anti-CD8 (53-6.7), anti-CD45.2 (Clone 104), PE-conjugated anti-CD4 (GK1.5), biotin-conjugated anti-TCRβ (597-H57), anti-CD5 (53-7.3) antibodies and Annexin V. Stained cells were analyzed on a Becton Dickinson FACScan flow cytometer using CellQuest software.

2.3. TCR-stimulation of thymocytes and splenic CD4-SP T cells

CD4-SP T cells were isolated by MACS using biotin-conjugated anti-CD4 antibody and streptavidin microbeads (Miltenyi Biotec). Freshly isolated thymocytes and CD4-SP splenocytes were incubated with anti-CD3 and anti-CD28 mAb (10 μg/ml each) for 20 min on ice and washed by ice-cold PBS followed by goat antihamster polyclonal antibody (40 μg/ml, Jackson ImmunoResearch Lab, West Grove, PA) and incubated for 2 or 5 min at 37 °C. Thymocytes and splenic CD4-SP T cells were lysed and analyzed by SDS-PAGE. Transferred membranes were Western-blotted with following the antibodies, anti-phopho-Erk, anti-Erk, anti-phospho-Akt (Ser473) and anti-Akt antibodies (Cell Signaling Technology, Beverly, MA). Detected proteins were visualized with ECL chemiluminescent substrate (Cell Signaling Technology).

2.4. Active Rac pull-down assay

Activity of Rac GTPases was measured by the standard p21-activated kinase (PAK)-binding domain assay. After 2×10^7 thymocytes were stimulated by TCR crosslinkimg, activated Rac protein was precipitated with p21-binding domain (PBD) beads (Upstate Biotechnology, Lake Placid, NY) and subjected to Western blotting analysis using Rac1- (23A8, Upstate Biotechnology), Rac2- (sc-96, Santa Cruz Biotechnology) or Rac3- [28] specific antibodies.

2.5. Labeling of CD4-SP T cells

CD4-SP T cells were labeled with 5(6-) Carboxyfluorescein diacetate N-succinimidyl ester (CFSE, Sigma, St. Louis, MO). Briefly, CD4-SP T cells isolated from spleen by MACS were resuspended at a concentration of 1×10^7 cells/ml in 5% FCS/PBS. Final concentration of 5 μM CFSE was added to the cell suspension. After a 5 min incubation period at 25 °C, the excess CFSE was washed by adding 5% FCS/PBS, and then resuspended in RPMI1640 containing 10% FCS.

2.6. Measurement of T cell growth in vitro

For proliferation assays, 96-well plates were coated with 0.1 ml of purified anti-CD3 (5 μg/ml) and anti-CD28 antibodies (5 μg/ml), and CFSE-labeled CD4-SP T cells were plated at a density of 2×10^5 cells and the culture was continued for 3 days at 37 °C. After incubation, CD4-SP T cells were analyzed on FACScan flow cytometor. For MTT assays, CellTiter 96® AQueous One Solution Cell Proliferation Assay kit (Promega, Madison, WI) was used. For survival assays, T cells were plated at a density of 1×10^6 cells/well in 96-well plates with or without 1 ng/ml IL-7 in a final volume of 200 μl/well.

2.7. Homeostatic proliferation analysis

Purified splenic CD4-SP T cells (2×10^6) from dnRac1-Tg or littermate control mice were injected into CD45.1, $RAG^{-/-}$ mice. Fourty days later, spleen, mesenteric lymph node and peripheral blood were harvested and cells were analyzed by FACS using, anti-CD45.2, anti-CD4 and anti-TCRβ antibodies.

2.8. Statistical analysis

Results are expressed as the mean ± S.E.M. of three independent experiments performed in triplicate. Student's *t*-test was used for multiple comparisons, and differences were considered to be statistically significant when the *p*-value was less than 0.05 or 0.01.

3. Results

3.1. Impaired differentiation of DP thymocytes in thymi of dnRac1-Tg mice

Both Rac1 and Rac2 are expressed in the thymus [1,20], however, expression of Rac3 in the thymus has not been characterized yet. We found low expression of Rac3 in the thymus by RT-PCR (Fig. 1A). However, we could not detect Rac3 protein by Western blotting using Rac3 specific antisera [28] (data not shown). Therefore, major Rac GTPases functioning in the thymus are Rac1 and Rac2. To investigate the precise function of Rac GTPases in T cell development and activation, we employed a dominant negative strategy which can suppress all three Rac GTPases [24]. We established dominant negative Rac1 transgenic (dnRac1-Tg) mice controlled by the human CD2 promoter containing the locus control region [29]. Expression of introduced HA-tagged dnRac1(N17) protein in the thymus of transgenic mice was detected as an upper band in Fig. 1B, which is also confirmed by Western blotting with anti-HA antibody (data not shown). As expected, TCR-induced activation of both Rac1 and Rac2 in dnRac1-Tg DP thymocytes was significantly inhibited (Fig. 1C).

The total number of thymocytes in dnRac1-Tg mice was decreased compared to littermate controls ($2.2 \pm 0.2 \times 10^8$ cells for controls; $1.5 \pm 0.1 \times 10^8$ cells for dnRac1-Tg). In dnRac1-Tg mice,

Please cite this article in press as: Sato Y, et al. Rac GTPases are involved in development, survival and homeostasis of T cells. Immunol Lett (2009), doi:10.1016/j.imlet.2009.03.014

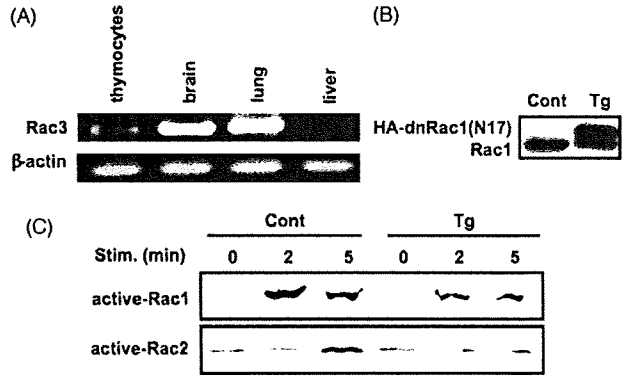

Fig. 1. TCR-induced activation of Rac1 and Rac2 was impaired in dnRac1-Tg mice. (A) RT-PCR analysis of Rac3 in the indicated tissues. (B) The expression of dnRac1N17 in total thymocytes isolated from dnRac1-Tg (Tg) and control (Cont) mice was detected by Western blotting with anti-Rac1. (C) Active Rac GTPases proteins were assayed by pull down with PBD beads from the lysates of total thymocytes with indicated stimulations and blotted with anti-Rac1 or Rac2 specific antibodies.

the proportion of CD4 CD8 double positive (DP) cells in the thymus was significantly decreased, while the proportion of double negative (DN) cells was increased (Fig. 2A and B). The ratio of DP to DN was strongly reduced, however, that of CD4-SP to DP was not changed, and the ratio of CD8-SP to DP was even slightly increased. For the calculation of the absolute number of mature CD8-SP in the thymus, we counted only TCRβ high cells in $CD8^+$ $CD4^-$ population to exclude immature CD8-SP. Absolute numbers of DN cells were normal in dnRac1-Tg mice and numbers of DP cells were decreased (Fig. 2C). From these results, transition from DN to DP, namely β-selection was significantly reduced in transgenic thymocytes. In transgenic mice, positive selection of CD4-SP was not affected, whereas positive selection of CD8-SP was slightly enhanced.

To confirm these results, we next investigated effects on positive selection using defined T cell receptor (TCR) specificity. We utilized class I restricted (OT-I) and class II restricted (OT-II) TCR transgenic mice, and crossed with dnRac1-Tg mice on a $RAG2^{-/-}$ background to avoid endogenous TCR rearrangement. As shown in Fig. 3, the ratios of DP to DN in both OT-I and OT-II were much less than controls, confirming impaired β-selection. In OT-II TCR Tg mice, the ratio of CD4-SP to DP is not reduced (Fig. 3B), indicating that positive selection of class II restricted TCR is not inhibited in the presence of dnRac1. In OT-I TCR Tg mice, the ratio of CD8-SP to DP was increased. This is consistent with the finding that generation of CD8-SP in the thymus is slightly increased by the inhibition of Rac GTPases.

3.2. Severe reduction of peripheral mature T cells in dnRac1-Tg mice

In thymi of dnRac1-Tg mice, we observed reduced numbers of CD4-SP T cells, but not of CD8-SP T cells (Fig. 2C), therefore, we next investigated subpopulations of peripheral mature T cells. As shown in Fig. 4, the proportion and absolute number of CD4-SP T cells in spleen of dnRac1-Tg mice were less than half of controls. The same magnitude of reduction was also observed in mesenteric lymph node (mLN) and peripheral blood (PBL). The reduction in the number of CD4-SP T cells in periphery was much severer than that observed in the thymus. Interestingly, the absolute numbers of CD8-SP T cells in spleen, mLN and PBL were also reduced in dnRac1-Tg mice (Fig. 4). In the thymi of dnRac1-Tg mice, the number of CD8-SP T cells was not reduced, therefore a reduction in the number of mature T cells in periphery cannot solely be attributed to the impaired generation of T cells in the thymus.

3.3. Increased apoptosis and impaired Akt phosphorylation in dnRac1-Tg mice

The reduced number of DP cells in the thymus of dnRac1-Tg could be a result of increased cell death, therefore we assessed spontaneous and TCR-induced apoptosis of DP cells by Annexin V staining. As shown in Fig. 5A, the proportion of Annexin V positive DP cells was slightly increased in dnRac1-Tg mice, whereas the proportion of apoptotic cells in DN, CD4-SP and CD8-SP cells were not altered. We next investigated the activation of Akt, evaluated by phosphorylation of residue Ser473 in the molecule, because Akt is known to be critical for the survival of DP cells [30–32]. In DP thymocytes, Akt is spontaneously phosphorylated without stimulation [31,33,34] and is further phosphorylated upon TCR-stimulation by anti-CD3 and CD28 antibodies (Fig. 5B). We found that spontaneous phosphorylation of Akt in freshly prepared thymocytes was absent in dnRac1-Tg mice. Furthermore, TCR-stimulation did not induce phosphorylation of Akt phosphorylation in the dnRac1-Tg thymocytes (Fig. 5B). On the other hand, TCR-dependent phosphorylation of Erk was completely normal in dnRac1-Tg thymocytes. From these results, we conclude that Rac GTPases are important for Akt activation with or without TCR stimulation, and thus critical in survival of DP cells, which is consistent with the recent results from a

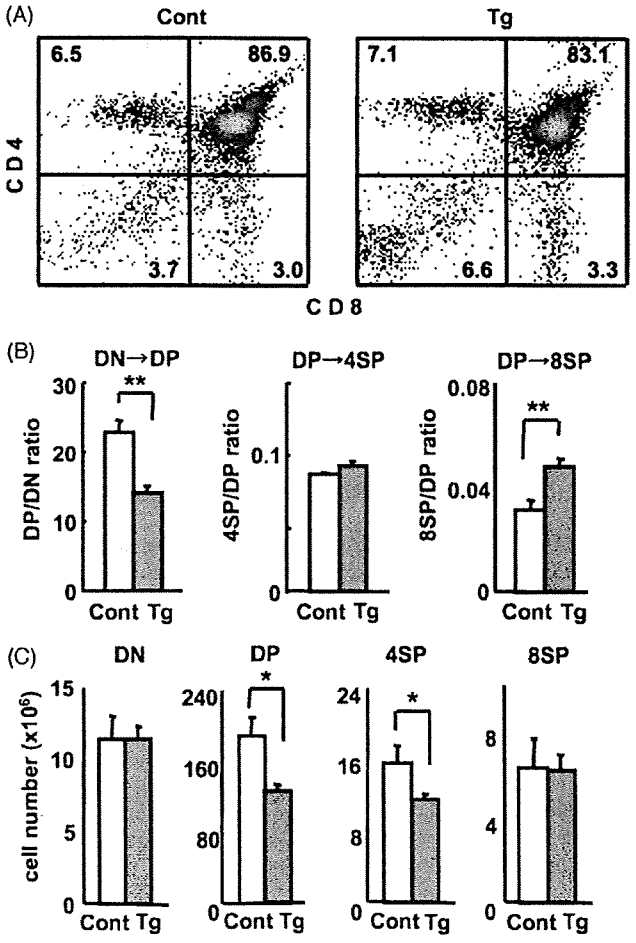

Fig. 2. Development of T cells in the thymus of dnRac1-Tg mice. (A) Thymocytes from 30-day-old dnRac1-tg mice and littermate controls were harvested. Expression of CD4 and CD8 in the thymus was analyzed by flow cytometry. (B) DP/DN, 4SP/DP and 8SP/DP ratios were calculated from analysis of dnRac1-tg mice (Tg) and littermate control mice (Cont). (C) Total cell numbers in DN, DP, CD4-SP and CD8-SP (TCRβhi) populations were calculated. Results are expressed as the mean ± S.E.M. of three independent experiments (Cont, $n = 8$; Tg, $n = 14$).

Please cite this article in press as: Sato Y, et al. Rac GTPases are involved in development, survival and homeostasis of T cells. Immunol Lett (2009), doi:10.1016/j.imlet.2009.03.014

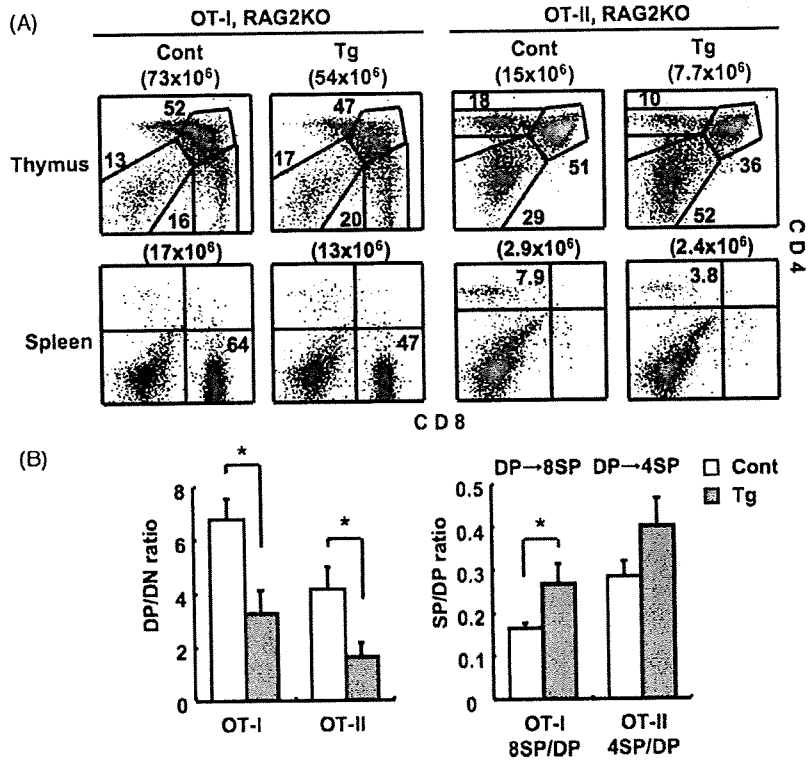

Fig. 3. Thymic selection of dnRac1-Tg expressing class I- and class II-restricted TCR transgenic mice. (A) The expression of CD4 and CD8 in the thymus and spleen of 30-day-old class I- and class II-restricted TCR transgenic, dn-Rac1-Tg mice (Tg) and littermate control mice. (B) DP/DN, 4SP/DN and 8SP/DP ratios of thymocytes were analyzed in class I- and class II-restricted TCR transgenic, dnRac1-tg mice and littermate control mice. The number of mature CD8-SP was calculated from $CD4^-$ $CD8^+$ TCR^{hi} gated cells. Bar graph data are expressed as the mean ± S.E.M. ($n = 3$).

conditional double knockout study of Rac1 and Rac2 in the thymus [22].

3.4. Increased spontaneous apoptosis in peripheral mature T cells

The decrease of mature CD4-SP T cells in periphery was much severer than that in the thymus, and the decrease of CD8-SP T cells was only seen in periphery but not in the thymus. Therefore, reduced numbers of peripheral T cells cannot be explained simply by the impaired survival of DP thymocytes in the thymus. We thus investigated the function of Rac GTPases in peripheral T cells. We first analyzed spontaneous apoptosis of splenic CD4-SP and CD8-SP T cells by the staining of Annexin V. As shown in Fig. 6A, the proportion of Annexin V positive cells of freshly isolated splenic CD4-SP and CD8-SP T cells in dnRac1-Tg mice was significantly increased compared to littermate control mice. At the same time, T cells with lower CD5 expression were significantly increased in dnRac1-Tg splenocytes (Fig. 6B). Since expression of CD5 on T cell is known to correlate well with the strength of TCR signal received [35], this result may indicate that mature T cells in dnRac1-Tg mice received a weaker TCR signal in vivo.

We next investigated Akt activation in splenic CD4-SP T cells. Spontaneous phosphorylation of Akt in splenic CD4-SP T cells without stimulation was reduced in dnRac1-Tg mice (Fig. 6C). Moreover, stimulation dependent phosphorylation of Akt was not detectable in dnRac1-Tg splenic CD4-SP T cells (Fig. 6C). As was seen in DP cells, TCR-induced phosphorylation of ERK was not altered in dnRac1-Tg CD4-SP T cells. These results suggest that Rac GTPases regulate tonic Akt phosphorylation in vivo, and are thus critical for survival of peripheral mature T cells.

3.5. Rac GTPases are required for homeostatic proliferation of mature CD4 T cells, but not for TCR-induced proliferation

We next investigated the effect of Rac GTPases on proliferation of mature T cells. Splenic CD4-SP T cells proliferate when stimulated with plate bound anti-CD3 antibody or a combination of anti-CD3 and anti-CD28 antibodies in vitro. As shown in Fig. 7A and B, TCR-induced proliferation after 3 days was nearly identical in both cell division evaluated by CFSE intensities and MTT assay. On the contrary, when CD4-SP T cells from dnRac1-Tg mice were transferred into lymphopenic $RAG2^{-/-}$ mice, homeostatic proliferation of mature CD4-SP T cells was significantly impaired compared to littermate controls (Fig. 7C). Because IL-7 is known to be critical in homeostatic proliferation under lymphopenic conditions, we next examined the IL-7-dependent survival of dnRac1-Tg T cells. Isolated splenic CD4-SP and CD8-SP T cells were cultured in vitro with or without IL-7 for 7 days and live cells were counted. Survival of both CD4-SP and CD8-SP T cells from dnRac1-Tg in vitro was not altered compared to control littermate (Fig. 7D). Addition of IL-7 in culture media rescued spontaneous cell death in vitro to some extent, however, the IL-7-dependent protective effect was THE same in dnRac1-Tg T cells. Therefore, we concluded that Rac GTPases are not involved in the IL-7 dependent survival of mature T cells. Collectively, these results suggest that Rac GTPases are important for survival and homeostasis of peripheral mature T cells.

4. Discussion

In the present study, we showed impaired generation of DP cells in the thymus and decreased number of peripheral T cells in dnRac1-Tg mice. The role of Rac GTPases in T cell development and activation has not been well characterized. Results from constitu-

Please cite this article in press as: Sato Y, et al. Rac GTPases are involved in development, survival and homeostasis of T cells. Immunol Lett (2009), doi:10.1016/j.imlet.2009.03.014

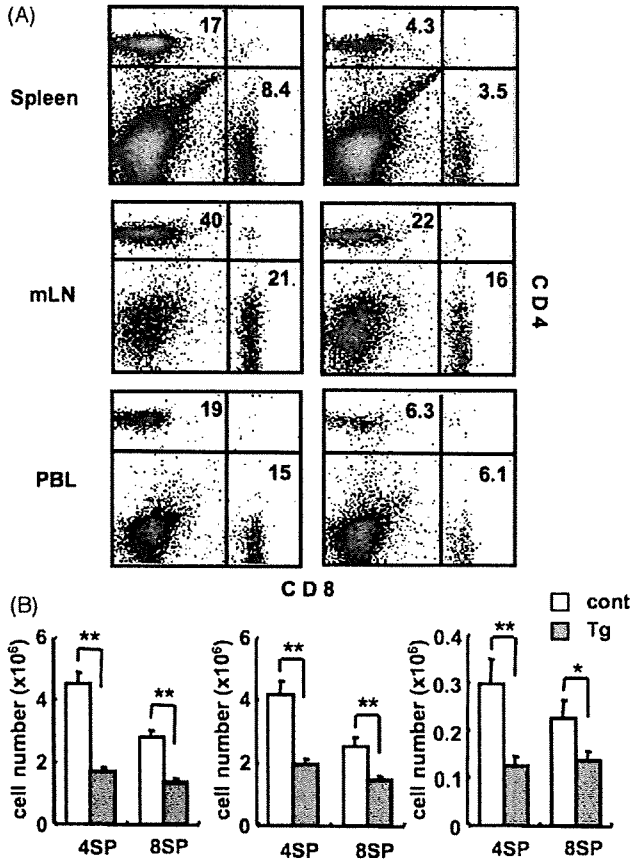

Fig. 4. Number of peripheral T cells is decreased in dnRac1-Tg mice. (A) T cells from spleen, mesenteric lymph node (mLN) and peripheral blood leukocytes (PBL) from 30-day-old dnRac1-Tg mice and littermate control mice were stained with anti-CD4 and anti-CD8 antibodies, and analyzed by flow cytometry. (B) Total cell numbers of CD4-SP and CD8-SP T cells from spleen, mLN and PBL were calculated on the basis of the percentages obtained by flow cytometry. FACS data represent one of four similar experiments for each experimental group. Bar graph of cell numbers are expressed as the mean ± S.E.M. of three independent experiments (Cont, $n = 17$; Tg, $n = 19$). $^{*}p < 0.05$; $^{**}p < 0.01$.

tively active Rac1 transgenic mice showing augmented TCR signal transduction [21], indicated that Rac1 is positively involved in TCR-dependent signal transduction in T cells. Moreover, a study using a DP cell line suggested that positive selection of CD4-SP required Rac1 [26]. From these previous results, we expected that defective Rac GTPases in the thymus would cause inhibition of positive selection.

However, surprisingly, positive selection in the thymus was not impaired in the dnRac1-Tg mice in vivo. Although total numbers of CD4-SP cells generated in the thymus were reduced in dnRac1-Tg mice, the CD4-SP to DP ratio was not altered, suggesting that positive selection of CD4-SP was not affected (Fig. 2). This was also confirmed when we specifically looked at the developmental fate of a class II specific TCR by analyzing the thymi of OT-II TCR Tg-dnRac1-Tg in RAG2$^{-/-}$ mice (Fig. 3). We even observed a slight increase of positive selection in CD8-SP, because the ratio of CD8-SP to DP was increased (Fig. 2). Again, this was also the case for the class I MHC specific OT-I TCR-Tg in RAG$^{-/-}$, dnRac1-Tg mice (Fig. 3). Therefore, reduction of the number of CD4-SP cells in the thymus was due to the reduction of DP cells, but was not due to impaired positive selection in the Tg mice. The reason why positive selection of CD8-SP is increased by inhibition of Rac GTPase activity should be revealed in future study.

Because of limitations in a dominant negative strategy, these phenotypes could be attributed to the insufficient inhibition of Rac GTPase activity (Fig. 1C), or to the unexpected effects by the inhibition of upstream guanine nucleotide exchange factors of Rac1. However, these results are consistent with those in Lck-Cre, Rac1$^{loxp/loxp}$; Rac2$^{-/-}$ mice, which were published recently [22]. Although deletion of either Rac1 alone [22] or Rac2 alone [17] did not affect T cell development, simultaneous deletion of Rac1 and Rac2 in the T cell lineage showed impaired T cell development. In lck-Cre Rac1/Rac2 double knockout (DKO) mice, numbers of total thymocytes were reduced to half, and numbers of CD4-SP cells but not of CD8-SP cells was reduced in the thymus. It was shown that positive selection of CD4-SP was not affected whereas positive selection of CD8-SP was increased. In the periphery of DKO mice, numbers of both CD4-SP and CD8-SP T cells were reduced. These phenotypes are almost identical to the one we saw in our dnRac1-Tg mice. Although we found very weak expression of Rac3 mRNA (Fig. 1A), Rac3 protein was unable to be detected by Western blotting (data not shown), therefore Rac1 and Rac2 are the major Rac GTPases in the thymus, and involvement of Rac3 would be negligible, if it ever exists. This is also consistent with the results that Rac1/Rac2 DKO mice showed similar phenotype to our dnRac1-Tg mice. Very recently, another group reported CD2-Cre driven Rac1/Rac2 DKO mice [23], whose

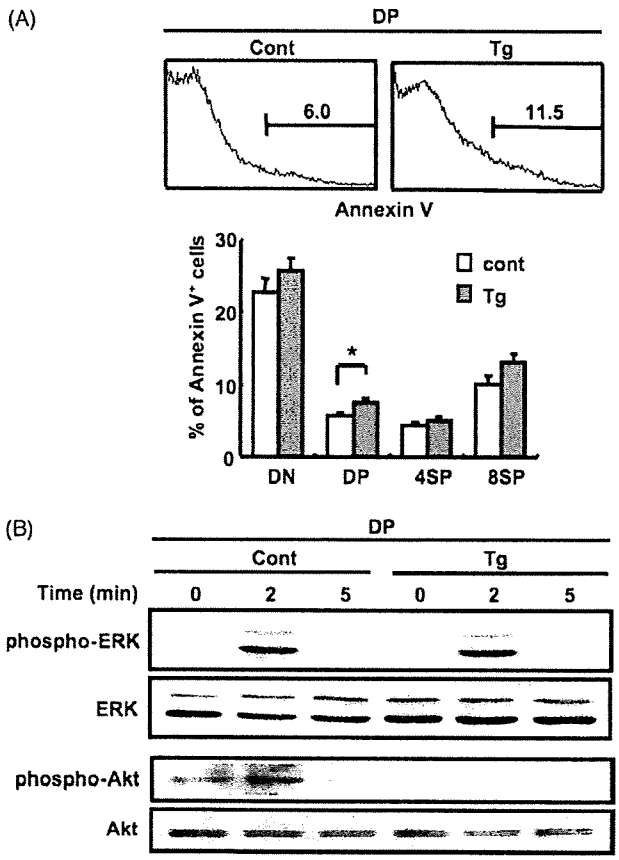

Fig. 5. Increased apoptosis and impaired Akt phosphorylation upon TCR stimulation in dnRac1-Tg DP thymocytes. Thymocytes from 30-day-old dnRac1-Tg mice (Tg) and littermate control mice (Cont) were stained with anti-CD4, anti-CD8 antibodies and Annexin V, and analyzed by flow cytometry. A, FACS data of Annexin V staining represent one of four similar experiments for each experimental group and bar graphs of Annexin V-positive cells were expressed as the mean ± S.E.M. of four independent experiments (Cont, $n = 12$; Tg, $n = 14$). $^{*}p < 0.05$; $^{**}p < 0.01$. (B) Thymocytes isolated from dnRac1-Tg mice were stimulated by anti-CD3 and anti-CD28 antibodies for the indicated periods. Cell lysates were analyzed by Western blotting with antiphospho-ERK, anti-ERK, antiphospho-Akt (Ser473) and anti-Akt antibodies.

Please cite this article in press as: Sato Y, et al. Rac GTPases are involved in development, survival and homeostasis of T cells. Immunol Lett (2009), doi:10.1016/j.imlet.2009.03.014

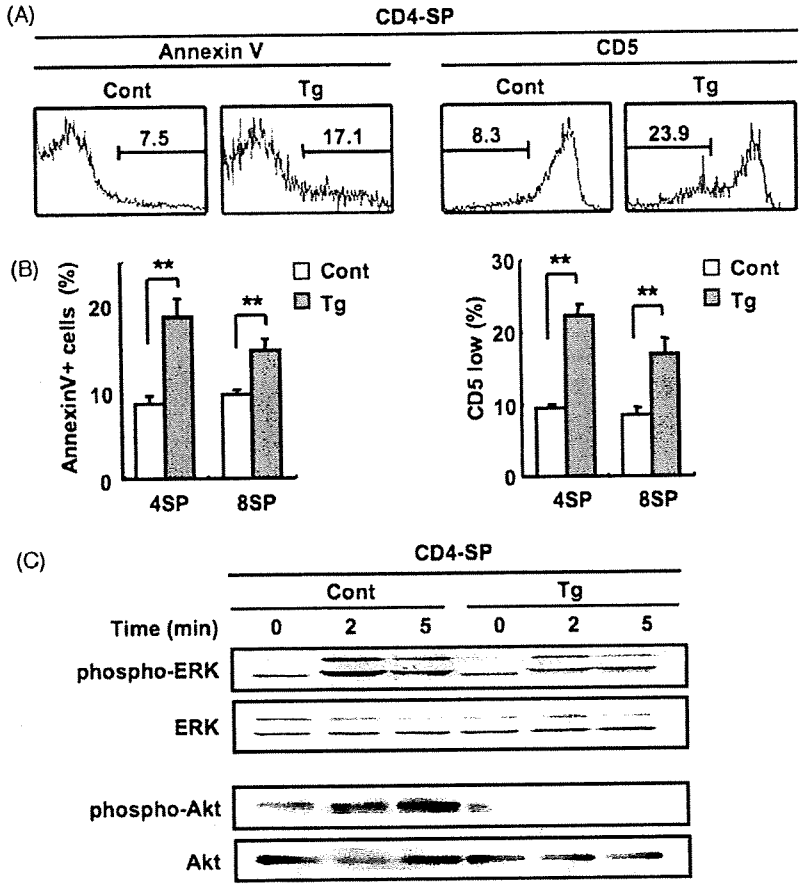

Fig. 6. Increased apoptosis and decreased Akt phosphorylation in dnRac1-Tg splenic T cells. T cells from spleen of 30-day-old dnRac1-Tg mice and nontransgenic littermate controls were stained with anti-CD4, anti-CD8 antibodies and Annexin V or anti-CD5 antibody, and analyzed by flow cytometry. (A) FACS data of Annexin V and anti-CD5 staining represent one of four similar experiments for each experimental group. (B) Bar graphs of indicating the percentage of Annexin V positive cells are expressed as the mean ± S.E.M. of four independent experiments (Cont, $n = 12$; Tg, $n = 14$). (C) Splenic CD4-SP T cells isolated from dnRac1-Tg mice (Tg) and littermate control mice (Cont) were stimulated with anti-CD3 and anti-CD28 antibodies for the indicated periods, and analyzed by Western blotting with antiphospho-ERK, anti-ERK, antiphospho-Akt (Ser473) and anti-Akt antibodies. $^{*}p < 0.05$; $^{**}p < 0.01$.

defect in T cell development was severer and earlier than the one in lck-Cre DKO. Our results is more similar to the phenotype in lck-Cre DKO than the one in CD2 Cre DKO.

We showed impaired spontaneous phosphorylation of Akt in dnRac1-Tg DP cells, and also defective Akt phosphorylation upon TCR stimulation (Fig. 5B). Akt signaling contributes to the differentiation process by promoting the survival of DP T cells [30,31]. This defective Akt activation is consistent with the results from the DKO mice for Rac1 and 2 [22]. These results suggest that the reduced numbers of DP cells seen in dnRac1-Tg mice could be at least partly because of increased cell death caused by impaired activation of Akt. We observed decreased numbers of mature CD4-SP and CD8-SP T cells in the periphery of dnRac1-Tg mice. The number of CD8-SP cells in the thymus was not reduced, and reduction of CD4-SP cells in the thymus was much slighter than that in the periphery, therefore, reduction of both CD4-SP and CD8-SP T cells in the periphery cannot simply be explained by developmental defects in the thymus. We observed increased apoptosis both in CD4-SP and CD8-SP T cells in periphery (Fig. 6A). We also noticed T cells with low CD5 expression were significantly increased in spleens of dnRac1-Tg mice (Fig. 6B), indicating that T cells from these mice received a weaker TCR signal in vivo. Furthermore, we showed that spontaneous activation as well as TCR-induced activation of Akt was severely decreased in dnRac1-Tg peripheral T cells.

Akt is a major downstream target of phosphatidylinositol (PI) 3-kinase signaling which is activated by various stimuli including TCR ligation [36–41]. Akt is activated by TCR stimulation and protects against cell death and regulate cell cycle progression in mature T cells [42]. Therefore, we think a major reason for the severe reduction of peripheral mature T cells in dnRac1-Tg is increased apoptosis caused by impaired Akt activation.

Proliferation and growth of dnRac1-Tg splenic CD4-SP T cells induced by anti-TCR antibody was not reduced in vitro, suggesting that TCR-dependent signal transduction is not seriously affected (Fig. 7A and B). Accordingly, TCR-dependent ERK activation was normal in dnRac1-Tg T cells (Fig. 6C). However, crosslinking of TCR by plate-bound antibody in vitro delivers artificially strong signals, so it may not represent the strength of signaling in vivo. Rac GTPases could be important in weak TCR signaling in vivo. We showed homeostatic proliferation by transferring dnRac1-Tg CD4-SP T cells into lymphopenic $RAG^{-/-}$ mice was significantly reduced compared to control mice. IL-7 and self-MHC molecules on antigen-presenting cells (APCs) play an essential role in the homeostatic expansion of peripheral naive T cells [43–47]. We showed that IL-7-dependent survival of mature T cells in vitro was not altered, suggesting that Rac GTPases are not involved in IL-7-dependent survival signal. Since Rac-dependent chemokine-promoted migration in vivo was shown to be important in homeostatic T cell survival and growth

Please cite this article in press as: Sato Y, et al. Rac GTPases are involved in development, survival and homeostasis of T cells. Immunol Lett (2009), doi:10.1016/j.imlet.2009.03.014